LABORATORY STUDY OF MECHANICAL AND HYDRAULIC PROPERTIES OF CEMENT–STONE DUST MIXTURES FOR INDUSTRIAL APPLICATIONS AND ROCK FRACTURE GROUTING

JADSADAKORN SRIPIYAPHAN

A Thesis Submitted in Partial Fulfillment of the Requirements for the
Degree of Master of Engineering in Civil, Transportation
and Geo-resources Engineering
Suranaree University of Technology
Academic Year 2023

การทดสอบคุณสมบัติเชิงกลและเชิงชลศาสตร์ของส่วนผสมหินฝุ่นกับซีเมนต์
สำหรับการประยุกต์ใช้ในงานอุตสาหกรรมและอุดรอยแตกหิน

นายเจษฎากร ศรีปิยะพันธุ์

วิทยานิพนธ์นี้เป็นส่วนหนึ่งของการศึกษาตามหลักสูตรปริญญาวิศวกรรมศาสตรมหาบัณฑิต
สาขาวิชาวิศวกรรมโยธา ขนส่ง และทรัพยากรธรณี
มหาวิทยาลัยเทคโนโลยีสุรนารี
ปีการศึกษา 2566

LABORATORY STUDY OF MECHANICAL AND HYDRAULIC PROPERTIES OF CEMENT-STONE DUST MIXTURES FOR INDUSTRIAL APPLICATIONS AND ROCK FRACTURE GROUTING

Suranaree University of Technology has approved this thesis submitted in partial fulfillment of the requirements for a Master's Degree.

Thesis Examining Committee
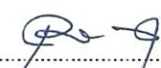
....
(Assoc. Prof. Dr. Pornkasem Jongpradist)
Chairperson

....
(Emeritus Prof. Dr. Kittitep Fuenkajorn)
Member (Thesis Advisor)

....
(Asst. Prof. Dr. Prachya Tepnarong)
Member

....
(Assoc. Prof. Dr. Yupaporn Ruksakulpiwat)
Vice Rector for Academic Affairs and Quality
Assurance

....
(Assoc. Prof. Dr. Pornsiri Jongkol)
Dean of Institute of Engineering

เจษฎากร ศรีปิยะพันธุ์ : การทดสอบคุณสมบัติเชิงกลและเชิงชลศาสตร์ของส่วนผสมหินฝุ่นกับ
ซีเมนต์สำหรับการประยุกต์ใช้ในงานอุตสาหกรรมและอุดรอยแตกหิน (LABORATORY STUDY
OF MECHANICAL AND HYDRAULIC PROPERTIES OF CEMENT–STONE DUST MIXTURES
FOR INDUSTRIAL APPLICATIONS AND ROCK FRACTURE GROUTING)
อาจารย์ที่ปรึกษา : ศาสตราจารย์ (เกียรติคุณ) ดร.กิตติเทพ เฟื่องขจร, 78 หน้า.

การศึกษานี้มีวัตถุประสงค์เพื่อประเมินศักยภาพในการนำหินฝุ่นมาใช้ประโยชน์ผสมกับ
ปูนซีเมนต์และ เบนโทไนต์ ผลการทดสอบชี้ว่าหินฝุ่นที่มีขนาดอนุภาคตั้งแต่ 0.25 มิลลิเมตรขึ้นไป
เหมาะสำหรับผสมกับปูนซีเมนต์ เนื่องจากให้ค่าความแข็งแรงในการกดอัดและความยืดหยุ่นใกล้เคียง
กับการผสมปูนซีเมนต์กับทรายละเอียด ส่วนหินฝุ่นที่มีขนาดอนุภาคต่ำกว่า 0.25 มิลลิเมตร เหมาะ
สำหรับงานกักเก็บน้ำ อัตราส่วนผสมระหว่างหินฝุ่นกับเบนโทไนต์ที่ 40% โดยน้ำหนัก แสดงผลการ
ทดสอบที่ดีที่สุด เนื่องจากให้ความหนาแน่นแห้งและค่าความต้านทานแรงเสียดทานสูงสุดขณะที่ใช้น้ำ
น้อยที่สุด ผลการทดสอบการบวมตัวยังสนับสนุนอีกว่า ส่วนผสมที่มีหินฝุ่น 40% มีอัตราการบวมตัว
ประมาณ 50% ของเบนโทไนต์บริสุทธิ์ อนึ่งการซึมผ่านของน้ำในหินฝุ่นมีแนวโน้มสูงขึ้นตามขนาด
อนุภาคที่ใหญ่ขึ้น การแบ่งแยกขนาดระหว่างหินฝุ่นหยาบและละเอียดที่ 0.25 มิลลิเมตร ช่วยเปิด
โอกาสให้นำหินฝุ่นไปใช้ประโยชน์ได้ทั้งในงานก่อสร้างและงานกักเก็บน้ำ

JADSADAKORN SRIPIYAPHAN: LABORATORY STUDY OF MECHANICAL AND HYDRAULIC PROPERTIES OF CEMENT-STONE DUST MIXTURES FOR INDUSTRIAL APPLICATIONS AND ROCK FRACTURE GROUTING.

THESIS ADVISOR: EMERITUS PROF. DR. KITTITEP FUENKAJORN, Ph.D., P.E., 78 PP.

Keyword: Stone dust/ Particle size/ Compaction bentonite/ Swelling capacity.

The objective of this study is to determine the potential applications of stone dust for cement and bentonite mixtures. Results indicate that stone dust with particle size ranges of 0.25 mm and larger is suitable for cement mixtures as they show compressive strength and elastic modulus values comparable to the cement- fine sand mixtures. The particle size ranges of 0.25 mm and finer are suitable for hydraulic containment applications. The weight ratio of stone dust to bentonite of 40% is recommended as its mixtures show the highest dry density, and frictional resistance with lowest optimum water content. Results from swelling test also support that at 40% stone dust content the swelling capacity of its mixtures is about 50% of that of pure bentonite. The permeability of stone dust is greater in larger particles. The separator between coarse and fine grained stone dust at 0.25 mm allows the application of stone dust to construction industry and hydraulic containment work.

School of Geotechnology   Student's Signature ....

Academic Year 2023   Advisor's Signature ....

ACKNOWLEDGEMENTS

I would like to express thanks to Emeritus Prof. Dr. Kittitep Fuenkajorn, thesis advisor, who gave a critical review. I appreciate his encouragement, suggestions, and comments during the research period. I would like to express thanks to Assoc. Prof. Dr. Pornkasem Jongpradist and Asst. Prof. Dr. Prachya Tepnarong for their valuable suggestions and comments on my research works as thesis committee members. Grateful thanks are given to all staffs of Geomechanics Research Unit, Institute of Engineering who supported my work.

Finally, I most gratefully acknowledge my parents for all their support and encouragement throughout the period of this study.

Jadsadakorn Sripiyaphan
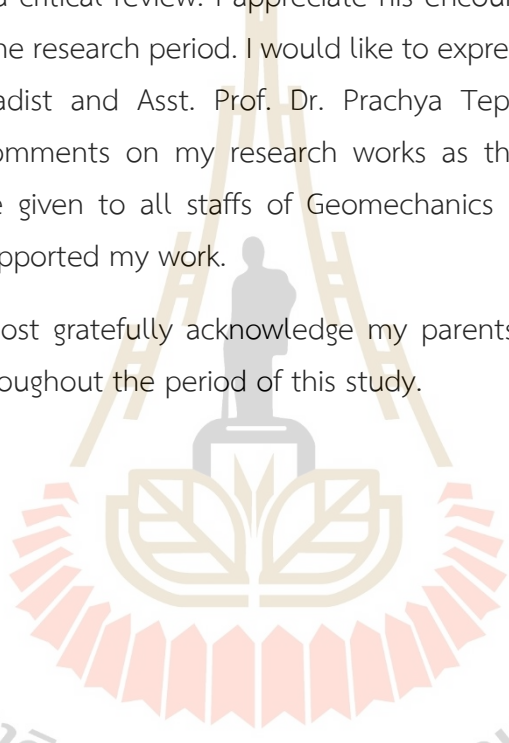
TABLE OF CONTENTS

<div align="right">Page</div>

TABLE OF CONTENTS (Continued)

TABLE OF CONTENTS (Continued)

TABLE OF CONTENTS (Continued)

LIST OF TABLES

LIST OF FIGURES

LIST OF FIGURES (Continued)

LIST OF FIGURES (Continued)

LIST OF FIGURES (Continued)

SYMBOLS AND ABBREVIATIONS

σ_c	=	Uniaxial compressive strength
E	=	Young's modulus
ν	=	Poisson's ratio
SD	=	Stone dust
C	=	Cement
B	=	Bentonite
ρ_{dry}	=	Maximum dry unit weight
ϕ	=	Angle of friction
σ_n	=	Normal stress
ε	=	Strain
XRD	=	X-ray diffraction
c	=	Cohesion
k	=	hydraulic conductivity
a_m	=	Internal cross-sectional area of standpipe
L	=	Length of soil sample
A	=	Sample area
t	=	Total time of discharge
h_1	=	Initial water level
h_2	=	Final water level
k_t	=	Coefficient of permeability for a test temperature of water at T°C
η_t	=	Viscosities at the temperature T°C of the test
η_{20}	=	Viscosities at the temperature 20°C of the test
h	=	Difference in head on manometers

CHAPTER I

INTRODUCTION

1.1   Background and Rationale

Stone dust is a waste product produced by limestone crushing plants during the process of producing coarse aggregates of various sizes. The workability, compressive strength, and optimum moisture content of stone dust with coarse particles is not significantly different from clean sand (Khamput., 2005). It is a good substitute material to reduce reserves and reduce the shortage of natural materials (Prakash and Rao, 2016) In an effort to optimize resource utilization, new applications for stone dust are being investigated to reduce stockpiling. These solutions include mixing stone dust with cement for use in the foundation, fill material (Satyanarayana, Varma, Chaitanya, and Raj, 2016), backfill material (Lee and Baek, 2023; Cai, Zhang, Shi, Chen, Chen, and Sun, 2020), flexible pavement (Satyanarayana, Prem Teja, Harshanandan, and Lewis Chandra, 2013), reinforced-stone dust walls (Sumitra and Mandal, 2015), construction materials such as brick block (Habib, Begum, and Salam, 2015) and ceramic tile fabricated (Tonnayopas, Kaewsomboon, and Jantaramanee, 2010). One established and widely used method employed in international construction practices to address permeability issues within fractured rock formations is grouting with a cement-bentonite mixture. The use of stone dust to minimize groundwater flow in rock fractures is another solution to the problem. Depending upon different regions in Thailand, stone dust is not truly acceptable in the locations where clean sand is vastly available (e.g., west and southeast of the country). Nevertheless, in the northeast of Thailand stone dust is well acceptable as a substitute of clean sand because the sand is not widely available. Care should, however, be taken to ensure that the particle size ranges, chemical compositions, particle shapes are suitable for substitution of the commonly used materials.

1.2   Research Objectives

The objectives of this study are to assess the mechanical of stone dust mixed with Portland cement and hydraulic properties stone dust mixed with bentonite for industrial use. The main tasks include particle size analysis, X-ray diffraction analysis,

uniaxial compressive strength tests, compaction tests, direct shear, consolidation tests, swelling test, and permeability test.

1.3   Scope and Limitations

The scope and limitations of this research include as follows.

1) The main focus of this research is to compare the mechanical behaviour of stone dust-cement mixtures and the hydraulic performance of stone dust-bentonite mixtures.

2) The particle sizes of the stone dust are 4.75 to 0.075 mm, as obtained from quarry in Nakhon Ratchasima Province.

3) Portland cement type I is mixed with stone dust following ASTM C150 (2012).

4) Uniaxial compression tests are performed of stone dust-mixed cement.

5) X-ray diffraction (XRD) is employed to identify the mineral composition according to ASTM E1426-14e1 (2019).

6) The sphericity and roundness are determined following the ASTM D2488-06 standard practice (2006).

7) The stone dust-to-cement (by dry weight) ratio of 2:1 is primarily selected.

8) Compaction tests of fined-aggregates stone dust-mixed bentonite are determined following the ASTM D1557-12.

9) Direct shear tests of fined-aggregates stone dust-mixed bentonite are determined following the ASTM D3080-11.

10) Consolidations tests of fined-aggregates stone dust-mixed bentonite are determined following the ASTM D2435 / D2435M - 11(2004).

11) Swelling tests are conducted on saturated bentonite samples at various weight ratios and under different vertical stresses.

12) The permeability test is performed on different particle sizes of stone dust.

1.4   Research Methodology

The research methodology is shown in Figure 1.1 includes literature review, samples collection, particles size analysis and classification, microscopic examination, mechanical properties tests, hydraulic properties tests, discussion, conclusion, and thesis writing.

1.4.1   Literature review

Literature review is carried out to study experimental research on the stone dust, particle size analysis, classification, mechanical and hydraulic properties. The source of information can be obtained from textbooks, journals, technical reports and conference papers.

1.4.2   Samples preparation

Stone dust samples used in this research have been collected from stone crushing plant, Nakhon Ratchasima province, Thailand. Stone dust samples are collected and sealed in moisture barrier bags. Preparation for testing then takes place at the Geomechanics Research Laboratory of Suranaree University of Technology. Nakhon Ratchasima province.
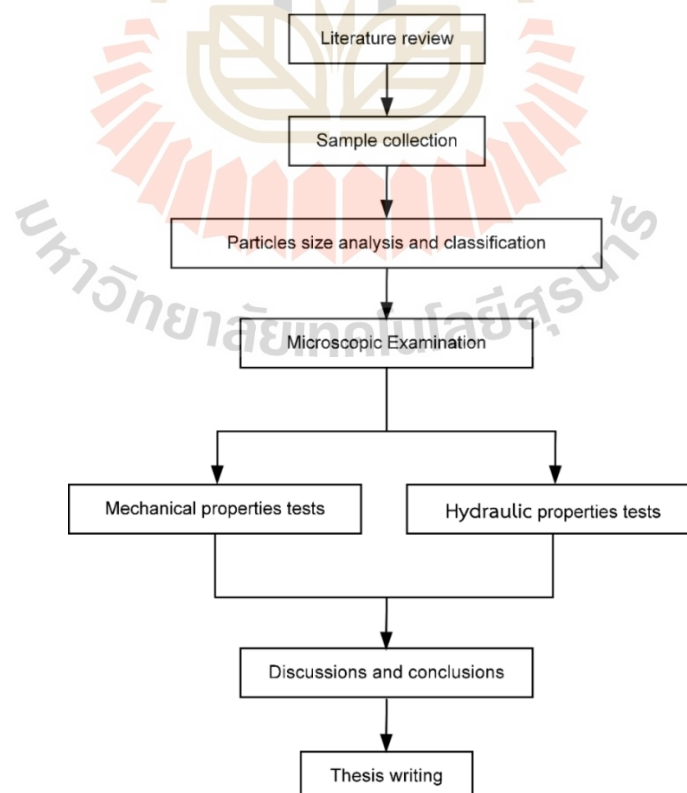
Figure 1.1 Research methodology.

1.4.3   Particle size analyses and classification

This investigation aims to identify the mineral composition of stone dust. X-ray diffraction analysis (using a Bruker D2 Phaser) will be conducted on samples of varying particle sizes to characterize and classify the stone dust, follow the ASTM E1426-14e1 standard practice. Minerals possess characteristic X-ray diffraction patterns, often referred to as 'fingerprints'. These patterns are archived within databases and employed by the DIFFRAC.TOPAS software to facilitate the identification of a material's composition.

1.4.4   Microscopic examination

The sphericity and roundness are determined from individual specimen in each size, follow the ASTM D2488-17e1 and used classification system given by Power (1982). The particle size of stone dust is observed using microscopic. Each size is scanned prior to testing mixed with cement.

1.4.5   Mechanical properties testing

1.4.5.1 Uniaxial Compressive Strength Test

The cement mixtures are divided into two stages. Stage I is to determine the maximum compressive strength of each particle size and stage II is implemented for ease of use in the industrial sector. The ranges of stone dust sizes for stage I are 4.75, 2.0, 0.85, 0.425, 0.25, 0.15 and 0.075-mm. In stage II the stone dust is separated into coarse and fine particles. Two sets of size separations are selected. Set I, particles within the ranges of 4.75-0.25 mm are considered coarse, while those within the range of 0.25-0.075 mm are classified as fine. Set II, particles sized 4.75-0.15 mm are considered coarse, and those within the range of 0.15-0.075 mm are classified as fine. During the test, axial and lateral displacements will be monitored. The obtained data will then be used to determine the elastic modulus and Poisson's ratio. In accordance with ASTM D7012-23 standard practice.

1.4.5.2 Compaction Test

Compaction tests are conducted on a range of particle sizes, from 0.25 mm to 0.075 mm. The weight ratios of bentonite to fine-grained stone dust mixtures investigated will be 100:0, 80:20, 60:40, and 40:60. The mixtures are prepared in a tray. The water is added to the mixture until the desired water content is reached. This testing procedure adheres to the guidelines established in ASTM D1557-12 for both the methodology and the corresponding calculations. Following the compaction tests, the data for dry densities and water contents are plotted. This analysis aims to

identify the combination that yields the maximum dry density and the optimal water content.

1.4.5.3 Direct Shear Test

Direct shear test is conducted using a direct shear device to determine the peak shear strength of the material. This test employs a vertical hydraulic load cell to apply normal stresses in increments ranging from 0.17 MPa to 0.69 MPa in a stepwise manner (0.17, 0.34, 0.52, and 0.69 MPa) The testing methodology and subsequent calculations adhere to the standards outlined in ASTM D3080-11. Following the test, the peak shear strength value will be employed to determine the material cohesion and friction angle through subsequent calculations.

1.4.6 Hydraulic properties tests

1.4.6.1 Consolidation Test

Consolidation test is conducted on compacted specimens comprised of bentonite-fine grained stone dust mixtures. The compaction process for each specimen utilizes its respective optimum water content. Specimens are then installed within a consolidation cell and subjected to constant stresses ranging from 10 kPa to 1280 kPa in a stepwise manner (10, 20, 40, 80, 160, 320, 640, and 1280 kPa). Each stress level is maintained for a duration of 10 days. The test methodology and subsequent data analysis are performed in accordance with ASTM D2435 / D2435M - 11(2004). The test results are employed to determine the axial strain, density, and void ratio of the specimens.

1.4.6.2 Swelling Test

To assess the swelling behavior under vertical stresses, a compacted mixture is subjected to a static load ranging from 2 to 6 kilograms in a stepwise manner. The test methodology and corresponding calculations adhere to the guidelines outlined in ASTM D4546-08 standard practice.

1.4.6.3 Permeability test

Permeability test employs standpipes of varying diameters (6 mm, 10 mm, and 13 mm) to determine the internal cross-sectional area for permeability calculations. Water flows from the standpipe through a compacted specimen contained within a mold having a diameter of 101 mm and a length of 122 mm. To ensure consistent permeability throughout the specimen, to achieve consistent compaction, the test material will be compacted in three layers of

approximately equal heights using a rammer. This procedure adheres to ASTM D2434-68 standard practices.

1.4.7 Discussions and conclusions

This section presents the key findings and compares the results of the different test conditions. By analyzing the data, the influence of varying stone dust particle sizes on the performance of the new material will be discussed. This evaluation aims to inform potential field applications of the stone dust-cement mixture.

1.4.8 Thesis writing

Comprehensive record of all research activities, methodologies employed, and the resulting data will be compiled and documented within the thesis. The research findings are intended for publication in either conference proceedings or peer-reviewed academic journals.

1.5 Thesis contents

Chapter I establishes the context of the research by outlining the background and significance of the problem. It will clearly define the research objectives, methodology, scope, and any limitations of the study. Chapter II provides a comprehensive overview of existing research relevant to the study. It summarizes the key findings and insights gleaned from the literature. Chapter III details the materials utilized in the research and the specific procedures followed for sample preparation. Chapter IV focuses on the mechanical properties of stone dust mixed with Portland cement, specifically in the context of construction applications and also outlines the laboratory testing procedures employed in the investigation, along with a presentation of the corresponding test results. Chapter V focuses on the hydraulic properties of stone dust mixed with bentonite for industrial use and outlines the laboratory testing procedures employed in the investigation. Presents a detailed analysis of the data obtained from the laboratory testing. Chapter VI provides a comprehensive discussion of the research findings, drawing conclusions based on the analysis of the data. It will also offer recommendations for future research endeavors in this area.

CHAPTER II
LITERATURE REVIEW

2.1　Introduction

Literature review is performed to increase understanding of topics studied. The literature review can be divided into related topics and summarized.

2.2　Effect of mechanical in cement mixture of stone dust

Stone dust (SD) finds frequent application in concrete production due to its widespread availability and cost-effectiveness. Many researchers (Priyanka and Dilip, 2013; Wakchaure, Shaikh, and Gite, 2012; Mahzuz, Ahmed, and Yusuf, 2011) have been find that solid wastes as an alternative material as fine aggregate include fly ash, slag limestone, waste plastic and SD. The literature review further indicates the potential of stone dust (SD) as a substitute for conventional cement concrete materials. Prior research has extensively investigated the influence of incorporating SD on the strength properties of cement concrete, specifically when utilized as a replacement for fine aggregate.

Suman (2018) investigated the use of SD as a partial replacement for fine aggregate in concrete. The proportion of materials containing cement, fine aggregate, coarse aggregate are 1:1.54:3, with a water-cement ratio of 0.42 and a superplasticizer dosage of 0.6% by weight of cement. Figure 2.1 presents the compressive strength results at 28 days, demonstrating that all concrete mixtures containing varying replacement levels of natural sand with SD exhibited strength exceeding the reference value. These findings suggest that SD incorporation can lead to beneficial outcomes in terms of concrete strength. Similar trends observed in the test results of Singh, Srivastava, and Agarwal (2015) further support the potential of SD for achieving both environmental and strength-related benefits.

Rajput (2018) finds alternative materials to fulfill the need for fine aggregate. Employed cement, coarse aggregate, and a combination of natural sand and stone dust

as fine aggregate materials are selected and water with no plasticizer. From Figure. 2.2, the results have shown that replacing natural sand with increasing amounts of SD leads to higher compressive strength in cement concrete compared to concrete made only with natural sand. This approach can also reduce waste materials generated by the mining industry.
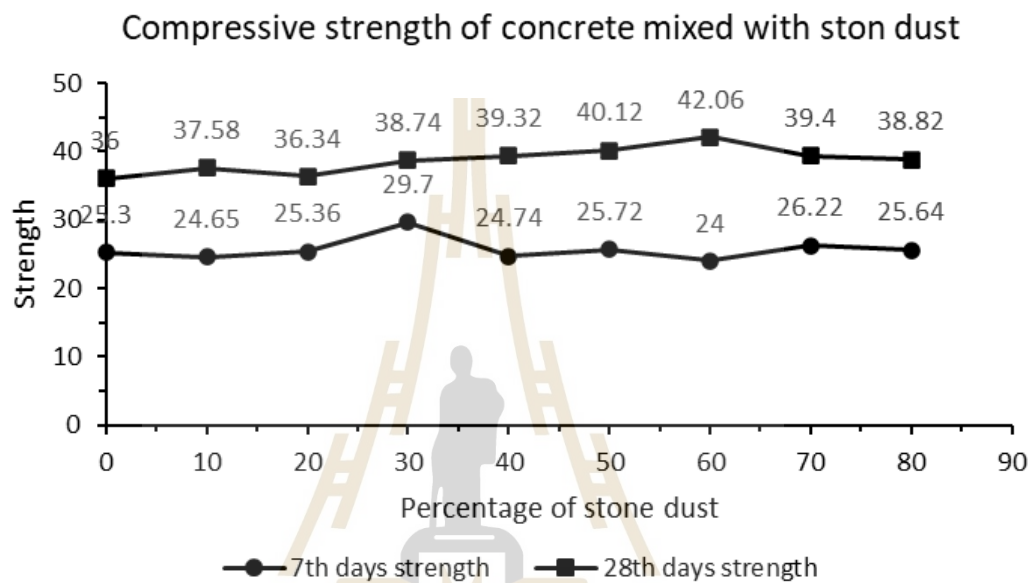
Figure 2.1   Variation of compressive strengths with gradual increase percentage of stone dust (Suman., 2018).
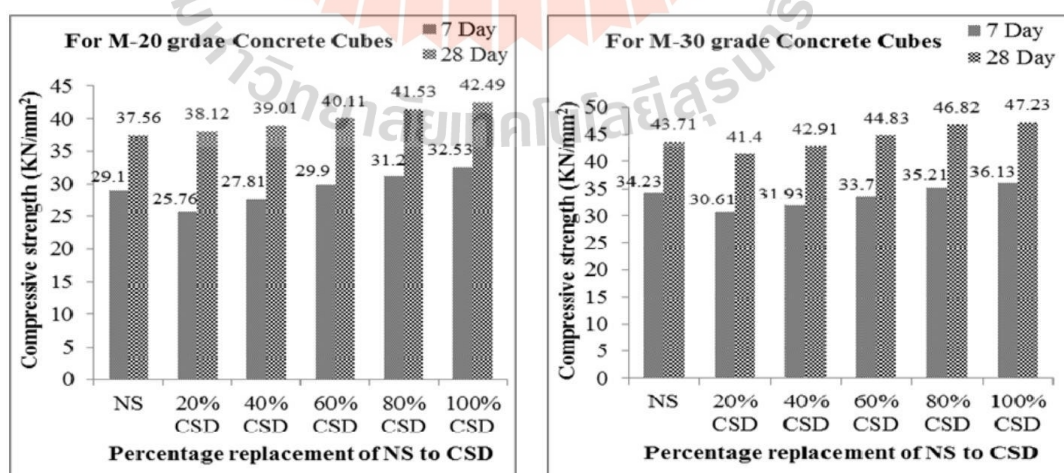
Figure 2.2   Compressive strengths of cement cube concrete with percentage replacement of NS to SD (Rajput., 2018).

Rajput and Chauhan (2014) study explore the use of stone dust as a fine aggregate in cement mortar, investigating its potential as a cost-effective alternative to river sand. The research findings indicate that stone dust can contribute to an increase in the compressive strength of cement mortars compared to those formulated with traditional river.

2.2.1 Effect of particle size

Yalley and Sam (2018) investigate the effects of fine sand content and water-to-cement ratio on concrete properties. Particle sizes range from 0.6 to 0.075 mm. They use fine sand contents of 2%, 4%, 6%, 8%, 10%, and 12% along with water-to-cement ratios of 0.55, 0.6, and 0.7. A basic 1:2:4 concrete mix is prepared. Their results show that concrete strength decreases significantly when the fine sand content exceeds 4% and the water-to-cement ratio is greater than 0.55. This might be because concrete with a higher fine sand content absorbs more water. To improve workability, it is recommended to limit fine sand content to 4% and use admixtures instead of increasing the water content.

Ghafoori, Spitek, and Najimi (2016) investigates the influence of limestone stone dust size and content on the compressive strength of self-consolidating concrete (SCC). by replacing 10, 15, and 20% of cement with limestone stone dust particles of 3 and 8 micrometers. As shown in Figure 2.3, the particle size distributions of limestone stone dust, cement, and fly ash indicate that both limestone stone dust particles are finer than those of Portland cement and fly ash. This allows them to act as fillers between cement particles, potentially improving the quality of the paste. Consequently, the compressive strength test results show an increase, likely due to the limestone stone dust filling the smaller voids between the cement particles. Thongsanitgarn, Wongkeo, Sinthupinyo, and Chaipanich (2011) also observe that increasing the amount of fine stone dust can increase concrete strength. They attribute this to two factors: (1) the very fine SD particles might act as nuclei for precipitation of Calcium Silicate Hydrate (CSH), thus increasing the degree of cement hydration, and (2) the increase in SD content and decrease in water content might reduce bleeding in the concrete mixes. For these reasons, to achieve good strength and reduce the risk of cracking, it is important to maintain a sufficient cementitious paste volume (Li and Kwan, 2015). On the other hand, Dhir, Limbachiya, McCarthy, and Chaipanich (2007) demonstrates that at equal water-to-cement (w/c) ratios, with equal cement and water contents, the strength of concrete mixes actually decreases as the limestone content increases. However, the differences between Portland limestone cement concrete

containing 15% limestone and Portland cement concrete are minimal, as shown in Figure 2.4. This finding aligns with the observations of many other researchers, who have shown that the compressive strength reaches a maximum value at a certain point and then decreases as the percentage of stone dust increases (Suman, Singh, and Srivastava, 2015; Prakash and Rao, 2016; Suman, 2018; Ali and Saikrishnamacharyulu, 2021).
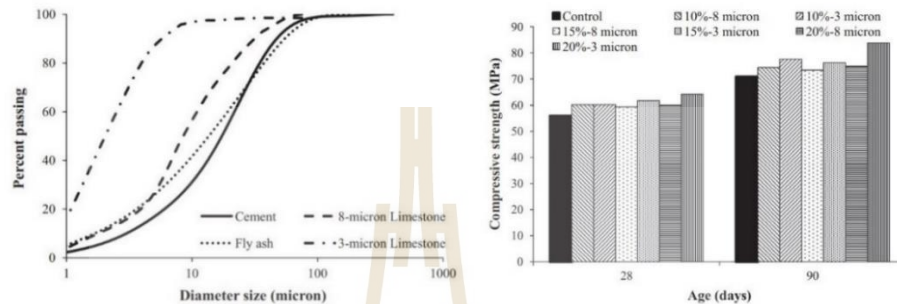
Figure 2.3   Particle size distribution of Portland cement, fly ash and limestone stone dust (left) and compressive strength of the selected SCCs (right) presented by (Ghafoori et al., 2016).
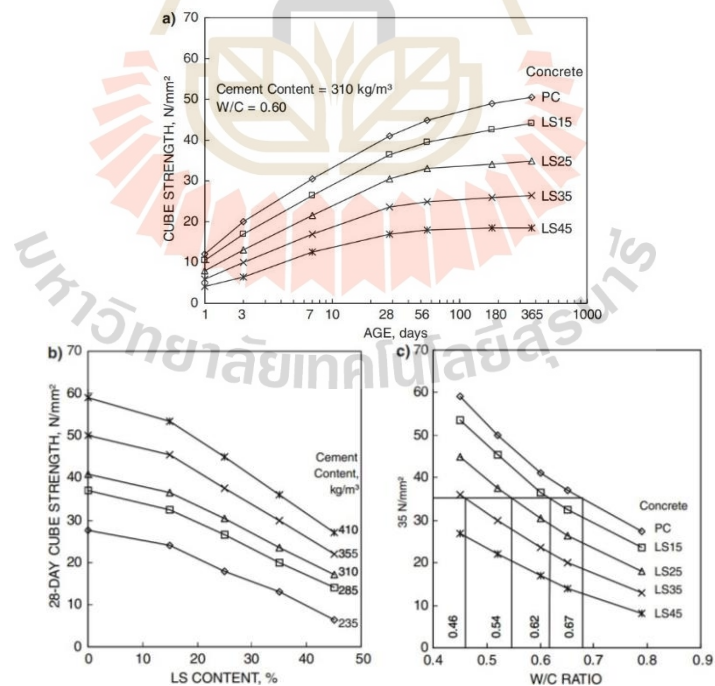
Figure 2.4   (a) Strength development and effect of (b) limestone content and (c) w/c ratio on 28-day cube strength of Portland cement and Portland limestone cement concretes (curing; 20°C water). (Dhir et al., 2007).

Neville (1995) describes how the use of a larger maximum size of aggregate affects strength in several ways. Because larger aggregates have less specific surface area and a weaker bond with the paste, failure occurs along the aggregate surfaces, resulting in reduced compressive strength of concrete. For a given concrete volume, using larger aggregates translates to a smaller volume of paste, which in turn provides more restraint to volume changes in the paste. This restraint can induce additional stresses in the paste, potentially creating microcracks before any load is applied. These microcracks can be critical factors in very high-strength concretes. Therefore, the general consensus is that using smaller sized aggregates is preferable for producing higher strength concrete.

Suwansukrot (2007) studies the effect of rock size on the compressive strength of concrete. They test concrete specimens made with Portland cement type 1 and water-reducing and accelerating additives. The compressive strength is measured at ages of 1, 3, 7, and 28 days, with 20 blocks tested at each age. Their results show that larger rocks exhibit higher compressive strength in the early stages (1 and 3 days). However, smaller rocks achieve greater compressive strength at later ages (7 and 28 days).

Haleerattanawattana (2004) studies the physical and mechanical properties of rock aggregates ranging from 3/8 inch to 1 inch in size. Finds that larger aggregates generally exhibit better physical properties compared to smaller ones. These properties include water absorption, unit weight, and the amount of void space between particles. In contrast, smaller aggregates tend to have a higher flakiness index (ratio of width to thickness) and elongation index (ratio of length to average thickness) than larger aggregates. For mechanical properties, however, the situation is reversed due to factors related to the crushing process. Smaller aggregates typically demonstrate higher strength, better compaction resistance, and greater resistance to erosion compared to larger aggregates.

2.2.2 Effect of particle shape

Neville (1995) describes the particle shape and surface texture are important external characteristics of aggregates. Roundness is a quantitative measure of a particle's relative sharpness, specifically its edges and corners. This property is primarily influenced by the inherent strength and abrasion resistance of the original rock from which the particle originates, as well as the extent of wear and tear it has undergone. When dealing with crushed aggregates, the final particle shape is determined by two key factors: the geological characteristics of the parent rock and the specific type of crusher employed, along with its reduction ratio (the degree to which the crusher diminishes particle size). Particle shape and surface texture influence the properties of freshly mixed concrete more than the properties of hardened concrete. The shape of fine aggregate particles influences the mix properties; angular particles requiring more water for workability. Coarse aggregate particles with equip-dimensional shape are preferred. Flaky particles affect adversely the durability of concrete because they tend to be oriented in one plane. The mass of flaky particles expressed as a percentage of the mass of the sample is called the flakiness index. Even though limits are not set down, the presence of elongated particles in excess of 10 to 15% of the mass of coarse aggregate is generally considered as undesirable (Dinku, 2005).

2.3 Application of stone dust mixture

Many researchers are reported that stone dust potential can be used as sub-base material in flexible pavements and embankment material (Satyanarayana et al., 2013), fill material (Singh et al., 2015), and road construction material (Pradeep, Satyanarayana, and Raghu 2013). Their potential can be supported as follow;

Lee and Baek (2023) studies the optimal mixing ratio for backfill material used in road excavation and restoration. By utilizing the entire amount of stone sludge generated during aggregate production. They analyze factors like flowability and material separation resistance to determine the ideal mix. The stone sludge used has a 100% passing rate on a 5-mm sieve and a 47.54% passing rate on a 0.075-mm sieve. Tests show that as the water-to-stone sludge-cement ratio increases, the flowability of the mixture improves, but the strength decreases. Among the tested, a stone sludge-cement ratio of 300% to 500% provides a satisfactory balance between flowability and strength for this application. Long-term monitoring conducted over approximately 5

months revealed no ground subsidence caused by traffic loads. Additionally, the backfill material proved to be suitable for re-excavation using standard equipment. Upon re-excavation, the team checked the filling properties around pipes and found no significant filling or damage to the pipes.

Prokopski, Marchuk, and Huts (2020) studies the use of granite dust in concrete mixtures as a way to utilize industrial waste in concrete production. This approach has the potential to reduce energy consumption and improve the quality of building materials. by creating standard cube samples and testing their compressive strength at various ages. The study also considers different mix proportions for the concrete. Findings show that the addition of granite dust accelerates the kinetics of concrete hardening, resulting in a faster rate of strength increase. This phenomenon can be attributed to the partial replacement of sand with dust, which leads to a more compacted microstructure in the cement matrix. This compaction is the main reason for the observed increase in concrete strength with the addition of dust. Overall, granite dust has a positive effect on both the early strength of concrete and the strength after longer curing periods, such as 90 and 180 days.

Satyanarayana (2016) describes natural soils containing plastic fines, such as silt and clay, can deform under heavy loads, potentially leading to failures. In geotechnical applications, crusher dust from crushing plants and river sand are commonly used to evaluate the performance of mixtures made with these materials. Compaction, compressive, and seepage tests are performed to assess the engineering properties of these mixes. The experimental data indicates that a mixture containing 60-70% crusher dust and river sand produces satisfactory results. This mixture is suitable for use as sub-grade and fill materials in various geotechnical construction projects. These findings align with the test results obtained by Sridharan, Soosan, Babu, and Abraham (2005, 2006) in their studies on quarry dust.

2.4 Effect of mechanical and hydraulic properties on bentonite and aggregate mixtures

2.4.1 Compaction

Charlermyanont and Arrykul (2005) study the compaction test on bentonite-sand mixtures to determine the optimal water content and maximum dry density. The results indicated that the dry unit weight of the bentonite-sand mixture rises with increasing water content. Once the optimal water content is reached, however, the dry unit weight diminishes with further water content increments. Consistently, augmenting the amount of bentonite leads to an increase in optimal water content and a decrease in maximum dry unit weight. Subsequent addition of water beyond the optimum content precipitates a significant decrease in the dry unit weight of the compacted bentonite-sand mixtures, particularly evident at high bentonite content. These findings align with those reported by Kaya and Durukan (2004) and Cai et al. (2020).

Srikanth and Mishra (2016) study the impact of sand content of a specific size on the behavior of bentonite-sand mixture across various ratios. Two bentonites of different mineralogical composition are selected for the study. These bentonites are named Bentonite 1 and Bentonite 2. They prepared different combinations of bentonite-fine sand (FS) and bentonite-medium sand (MS) by adjusting the sand content from 50 to 90 % by the dry weight of the mixture. Bentonite-FS and bentonite-MS mixtures demonstrated distinct optimal water content and maximum dry density values, suggesting a potential influence of sand particle size on compaction characteristics. Mixtures containing MS exhibited comparatively higher maximum dry density and lower optimal water content values for both type of bentonites, likely due to the effective packing of bentonite particles within the void spaces formed among the sand particles.

The behavior of bentonite-sand mixtures depends on the of bentonite content. With a low bentonite content, the mixture retains the characteristics of granular soil. However, as the bentonite proportion increases, there's a gradual transition of the mechanical properties typical of plastic clay. This interaction between bentonite and sand is using Scanning Electron Microscopy (SEM), as shown in Figure 2.5, it reveals bentonite particles adhere to the surface of sand grains, forming "bridges" that connect the larger particles. (Proia, Croce, and Modoni, 2016).
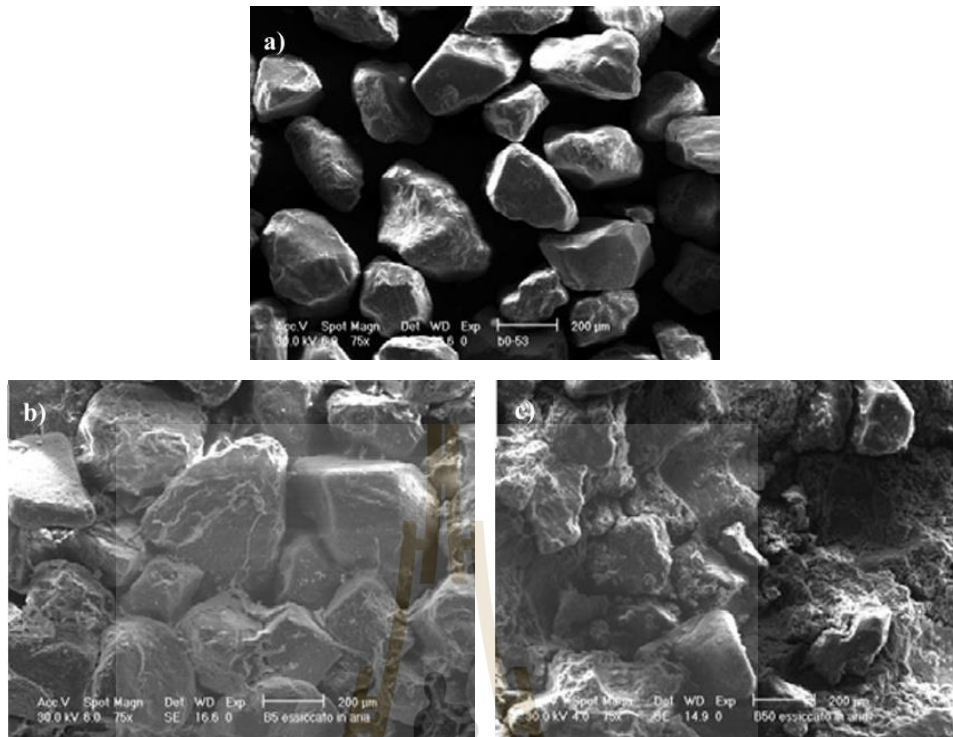
Figure 2.5 SEM of dried samples at magnification factors of 75x; a) with sand 100%,

b) with bentonite 5%, and c) with bentonite 50% (Proia et al., 2016).

2.4.2   Direct shear test

Yanrong (2013) investigates the shape and size variation of particles affect the shear behavior of composite soils containing a broad spectrum of particle sizes. Two sets of comparable samples are created: (1) a combination of fine particles (clay and silt) with a perfectly shaped coarse fraction (glass sand and beads), and (2) a combination of fine particles with a naturally occurring coarse fraction (river sand and crushed granite gravels). The results showed that an increase in the proportion of coarse particles led to a higher constant volume shear strength. Additionally, as the elongation of the coarse particles increased, or their convexity decreased, the constant volume friction angle also increased. The overall roughness of the shear surface, when the volume remains constant, has a negative correlation with the smoothness (convexity) of the particles and a positive correlation with the area of the shear surface occupied by particles of specific shapes. To quantify the particle shape, two parameters, convexity and elongation, are derived from 2D images of the soil particles. As shown in Figure 2.6.

The relationship between shear strength and particle size is then analyzed by Bagherzadeh-Khalkhali and Mirghasemi (2009). The results indicate that samples with larger maximum particle sizes exhibit greater shear strengths. This is because the value of the shear parameter is dependent on the size of the grains. while the friction angle increases as the grain size increases, as confirmed by research from Soltani-Jigheh and Jafari (2012), and Kim and Ha (2014).

Vangla and Latha (2015) investigate the influence of particle size distribution on the shear behavior of sand. Their symmetric direct shear tests revealed that particle size itself does not affect the peak friction angle when the tests are conducted at the same void ratio. However, the ultimate friction angles are impacted by particle size, with larger particles exhibiting higher ultimate friction angles. Figure 2.7 shows the shear stress and displacment response of the sands is influenced by their angularity. Increased angularity resulted in higher peak shear strength due to an enhancement in interlocking forces between the particles. It's important to note that the sands had relatively similar angularity and roundness properties. This suggests that the morphological effects are negligible, and the observed variations in shear behavior are primarily due to differences in particle size. This aligns with the findings of Holtz and Kovacs (1981), who reported that particle size has no effect on the peak friction angle if the void ratio remains constant.

Circularity	1	0.47	0.89	0.52	0.47	0.21
Convexity	1	1	1	1	0.70	0.73
Elongation	0	0.82	0	0.79	0.24	0.83

Figure 2.6 Illustration of particle shape parameters (Yanrong, 2013).
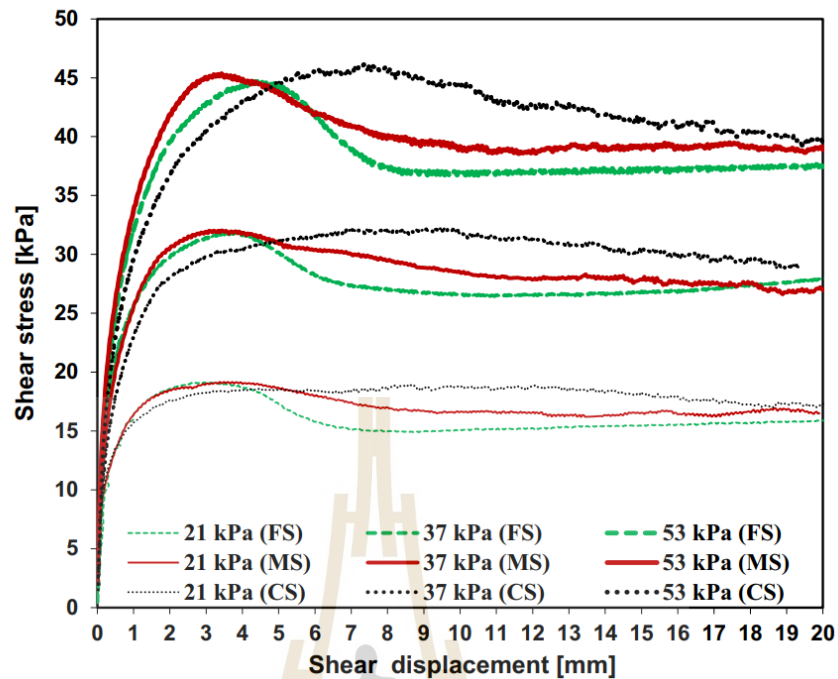
Figure 2.7   Shear stress versus shear displacement response of different sands (Vangla and Latha, 2015).

2.4.3 Consolidation test

Duong and Hao (2020) study the consolidation characteristics of artificially structured bentonite-kaolin mixtures with different pore fluids. Oedometer tests are conducted on bentonite-kaolin mixtures containing 10%, 20%, and 30% bentonite content. Distilled water is used as pore fluids. Samples are consolidated to create an "artificial structure". Bentonite significantly impacts the consolidation behavior of mixtures. Compression index, swelling index, and coefficient of volume change increased with increasing bentonite content.

Pastor, Tomás, Cano, Riquelme, and Gutiérrez. (2019) study the improvement of clayey soils by using limestone dust addition. All the samples are compacted at 0, 5, 10, 15, 20, and 25% of limestone dust. Tests are one-dimensional consolidation tests conducted under the loading sequence of 5 up to 800 kPa and unloading sequence of 400 up to 20 kPa. From the test result, increase in the stiffness of the clayey soil by 27% when 25% limestone dust is added. The compression index, which is a direct indication of the tendency of a clayey soil to settle when it is loaded, decreases as the amount of additive increases. A similar trend is observed for swelling

index with a maximum reduction of 31% when 25% of limestone dust is added. This lower compressibility of the mixed clayey soil is attributed to the fine aggregates of the limestone stone dust filling the voids of the clayey soil. This agrees reasonably well with the test results obtained by Mishra et al. (2010) who study the effect of the physical, chemical and mineralogical properties on the 15 different bentonite-soil mixtures.

2.4.4 Swelling test

Pastor et al. (2019) describe the effect of adding limestone dust on the free swelling of the soil. The result found that the swelling index reduced from 5.7% to 3.38% when only 5% of limestone dust is added. This constitutes a reduction of 42% in the swelling index of the mixed soil. Reductions of 58%, 61%, and 56% are observed when the limestone stone dust addition is 10, 15, and 20%, respectively. The results are consistent with previous research (Saygili, 2015; Sabat and Nanda, 2011), show a decrease in the swelling index with increasing marble dust up to the maximum amount. Ogila (2016) report that a decrease between 30 to 45% of the heave percentage of swelling index when 20% of limestone dust is added to clayey soils, similar to results obtained by Sabat and Muni (2015). The increase of the swelling index while 25% limestone stone dust addition is due to the significant increase in matric suction caused by the reduction in the initial water content of the samples. This is because the stone dust is added dry to the wet soil.

Srikanth and Mishra (2016) indicate that compacted bentonite-soil mixtures are utilized in waste disposal and nuclear waste sites. The particle size of sand in bentonite mixtures affects their behavior, with fine sand mixtures displaying higher shrinkage limits. Mixtures with medium sand have higher density and lower water content. Sand content influences engineering properties, with fine sand mixtures showing higher liquid limits and swelling pressure. Additionally, fine sand mixtures exhibit lower hydraulic conductivity due to effective void filling. The result indicate that bentonite content below 20% is insufficient for filling void spaces. The results similarly with of Bilal and Ahmad (2020) who study the soil swell potential on bentonite-stone dust mixtures. When used the stone dust in range of 10, 20, 30, 40 and 50% and concluded that only 30% is enough to improve soil properties. The reason why stone dust improves soil properties is that it possesses a pozzolanic nature and contains coarse particles that improve compaction characteristics and reduces the plasticity. Moreover, it has good interlocking strength with soil because of its angular shape.

2.5 Permeability properties of stone dust

Akbulut and Cabalar (2014) study the effects of physical properties of sand (e.g., size and shape) on the hydraulic conductivity. Five materials with different sizes and particle shapes are used in this study. By permeability testing apparatus is employed for the experiments. The experimental results show that relatively rounded sand grains have decrease hydraulic conductivity values than the angular sand grains. This is because increase particle rotation allows for a more open fabric in angular sand grain samples compared to rounded ones. Consequently, more angular sand exhibit higher hydraulic conductivity values. According to by Cedergren (1989) and Sperry and Peirce (1995) show that particle shape affects both permeability and liquefaction potential. Horak, Sebaaly, Maina, and Varma (2017) shows this concept by zooming in on the voids of the three levels consecutively filled with smaller and smaller aggregate grading groupings. This allows for clear visualization of the main structural elements within each consecutively smaller of the grain matrix, without the influence of finer aggregates filling the voids. The latter mainly provide stability to this grain matrix (Figure 2.8).
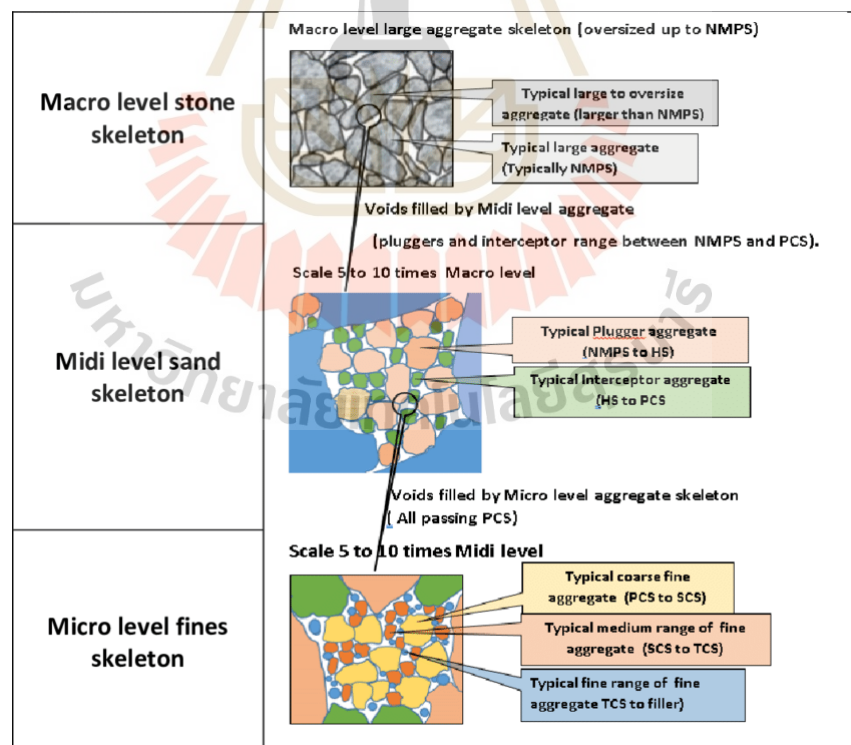
Figure 2.8   Three level grain matrix infill illustration (Horak et al., 2017).

2.6   Weight ratio of bentonite-stone dust mixture

Jain, Jha, and Akhtar (2022) describes marble dust (MD) as a viable alternative to sand (S) when mixed with bentonite (B). Microstructural images with 20% bentonite content show the filling and coating of bentonite particles within the inter-particle voids and on the surface of the sand and marble dust particles. This process transforms the coarse-grained matrix into a coarse-grained cohesive matrix (Fig. 2.9 c and f). Furthermore, a 40% bentonite content induces the adherence of bentonite particles on the surface of sand and marble dust particles, thereby forming a compacted matrix (Fig. 2.9 b and e). However, with a higher bentonite content of 60%, the sand and marble dust particles become noticeably immersed within the bentonite matrix. Based on this preliminary assessment, optimal results are achieved when sand or marble dust constitutes less than 40% of the mixture, indicating a requirement for a higher bentonite content for developing landfill liners. This aligns report by Pusch (1998) that a 30% bentonite content is effective for backfill applications. The recommendations by Sobti and Singh (2017) for optimal barrier material compositions are as follows: sand-bentonite with 10% bentonite content, coal ash-bentonite with 10% bentonite content, and silt-bentonite with 5-10% bentonite content. It is important to note that a 5% bentonite content for sand and coal ash mixtures may not be sufficient, as indicated by the higher hydraulic conductivity (k) value observed in these cases. On the other hand, a stone dust content of 20-30% is sufficient to improve soil properties. The reason stone dust enhances soil properties is that it possesses pozzolanic characteristics and contains coarse particles, which improve compaction characteristics and reduce plasticity. Moreover, it has good interlocking strength with the soil due to its angular shape.
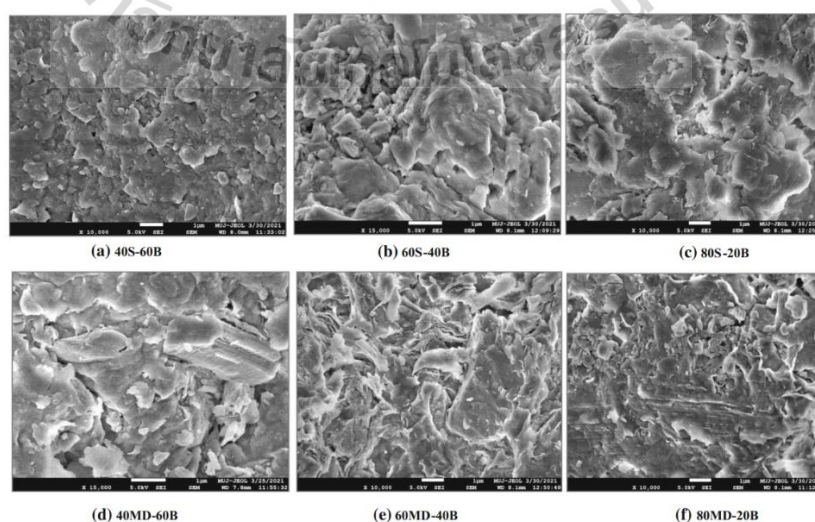
Figure 2.9 Microstructural examination of S–B and MD–B mixes Jain et al. (2022).

CHAPTER III
SAMPLE PREPARATION

3.1   Introduction

This chapter describes basic characteristics of stone dust used in this study. The limestone stone dust deposits and description are described.

3.2   Rock Description

Stonedust samples used for testing are limestone obtained from Khum-ngern Khum-tong Co., Ltd., stone crushing plant, Nakhon Ratchasima province. It belong to Permian sequences, characterized by predominantly thick carbonate sediments, and are extensively distributed throughout the country. They are classified as part of the Ratburi Limestone Formation or Ratburi Group, with the type locality situated in Ratchaburi province, western Thailand (Brown et al., 1951; Javaaphet, 1969). Bunopas (1981) proposed restricting the designation 'Ratburi Group' to Permian limestones found in western and peninsular Thailand. He introduced the term 'Saraburi Group' to encompass Permian limestones and clastic rocks in central and northeastern Thailand. This distinction is justified by the significant faunal disparity between the Ratburi Group, deposited in the peri-Gondwana realm, and the limestones of the northeast, including the current study area, which originated within the Tethyan realm.

3.3   Sample preparation

The stone dust used in this study is prepared from Khum-ngern Khum-tong Co., Ltd., stone crushing plant of the Saraburi group in Nakhon Ratchasima province. Sieve analysis is employed to determine the particle size distribution of the specimens, with the results presented in Figure 3.1. The bulk density of the specimens, defined as the ratio of dry mass to volume, is determined to be 1.62 g/cc in accordance with the ASTM C29/C29M-23 standard. Mineral composition analysis of the specimens is conducted using X-ray diffraction (XRD). To prepare the samples for XRD analysis, the stone dust is crushed into a rock powder with particle sizes less than 0.25 mm (mesh #60).

The XRD analysis is performed using a Bruker D2 Phaser instrument, adhering to the guidelines outlined in ASTM E1426-14 standard practice. The results of the XRD analysis are summarized in Table 3.1.

The sphericity and roughness of individual particles are evaluated across 7 particle size ranges: 4.75 mm, 2.0 mm, 0.85 mm, 0.425 mm, 0.25 mm, 0.15 mm, and 0.075 mm. Ten particles are examined within each size range using an optical microscope (as shown in Figure 3.2). Following the established classification systems outlined by Powers (1982) (Figure 3.3), the average roughness and sphericity values for each material are presented in Table 3.2.
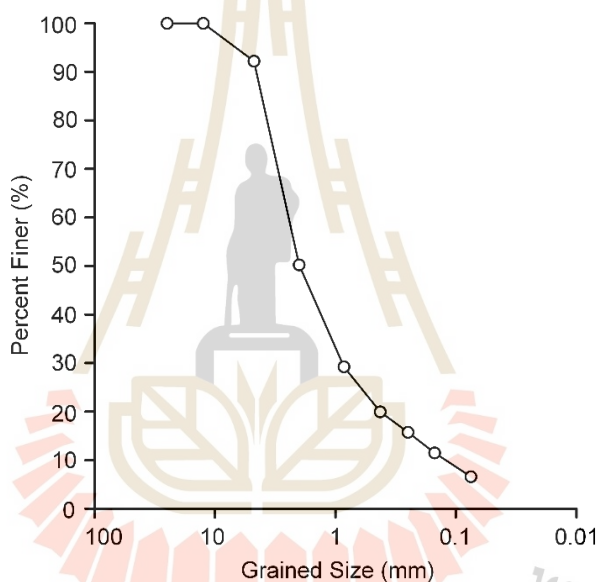
Figure 3.1 Particle size distributions of stone dust.

Table 3.1 Mineral compositions from XRD analysis.

Mineral Compositions	Concentration (%)
Calcite	66.92
Dolomite	25.97
Ankerite	3.51
Huntite	1.61
Cooperite	0.18
Cuspidine	1.12
Natron (Soda)	0.69
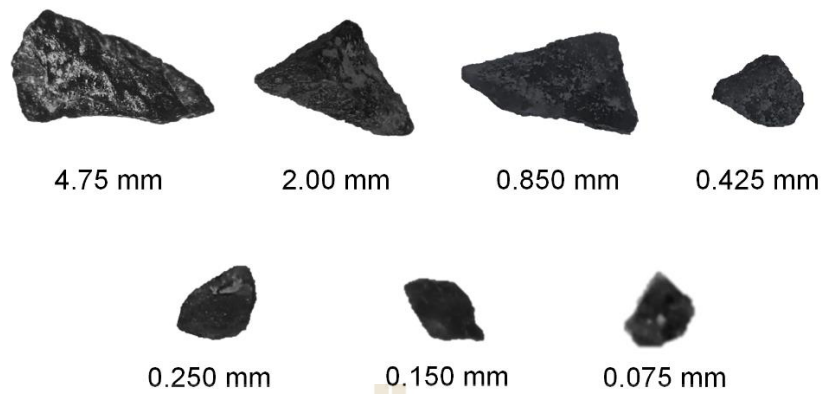
Figure 3.2 Examples of representative size and stone dust particles.
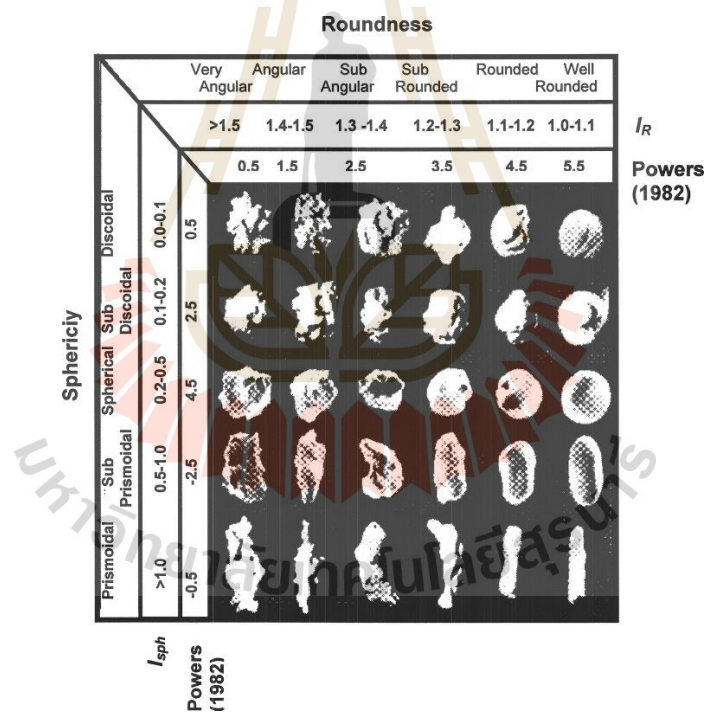
Figure 3.3   Estimation of roundness and sphericity of sedimentary particles

(Powers,1982).

Table 3.2   Particle shape classification of stone dust particles based on Powers (1982).

Particle size (mm)	Roundness	Sphericity
4.75	0.37	0.48
2.0	0.46	0.77
0.85	0.51	0.57
0.425	0.43	0.80
0.25	0.49	0.91
0.15	0.41	0.77
0.075	0.74	1.00
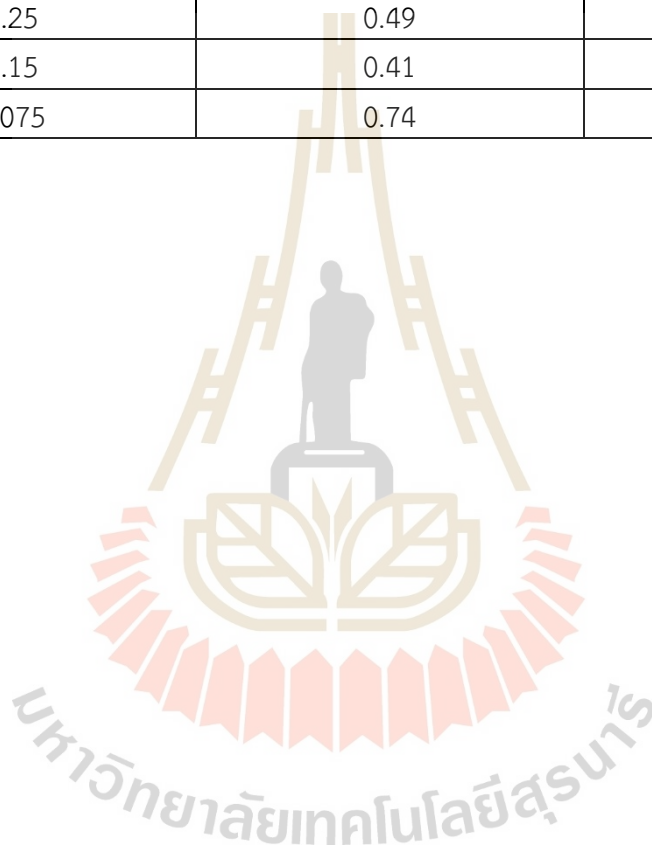
CHAPTER IV
MATERIAL CLASSIFICATION AND LABORATORY TESTING

4.1   Introduction

This chapter describes a method to separate the stone dust into various size ranges. Each size range is mixed with cement. The mixing ratio (e.g. water, cement and aggregate (stone dust)) follows relevant ASTM standard practice. Compressive strength and elastic parameters are used as indicators to decide the appropriate particle size range to be used for cement mixing application or to be used for hydraulic containment application. Cement mixing with clean sand is also performed to compare its mechanical properties with the stone dust cement mixtures.

4.2   Grains size classification

4.2.1   Sieve analysis

The stone dust particle sizes are classified using sieve nos. 4, 10, 20, 40, 60, 100 and 200. Cumulative curves are constructed based on weight percent. The test method and calculation follow the ASTM C136–06 standard. Figure 4.1 shows the results. The stone dust sizes are similar to clean sand. Their weight percents are classified based on Unified Soil Classification System (USCS), as shown in Table 4.1.

The stone dust for specific size range is mixed with cement to determine the mechanical properties of each mixture. The cement mixtures are divided into two stages. The ranges of stone dust size for stage I separation are given in Table 4.2, to obtain the mixture properties under all size ranges. They are also shown on the particle size distribution curve in Figure 4.2. Results from stage I testing could reveal the detail of effect of aggregate sizes on the mixture strength. For stage II testing, the entire particle size range is separated into 2 parts, as shown in Table 4.3 and Figure 4.3. Set I, particles within the ranges of 4.75-0.25 mm are considered coarse, while those within the range of 0.25-0.075 mm are classified as fine. Set II, particles sized 4.75-0.15 mm are considered coarse, and those within the range of 0.15-0.075

mm are classified as fine. This is primarily to be more practical and economic for the industry, where only one separator is required at the end of the conveyer belt that carries the stone dust from the rock crusher. In the study, two sets of size separations are used. (0.25-0.075 mm and 0.15-0.075 mm). The mixture strength will be used as an indicator of which size separators would be more appropriate between strength application and hydraulic containment application.
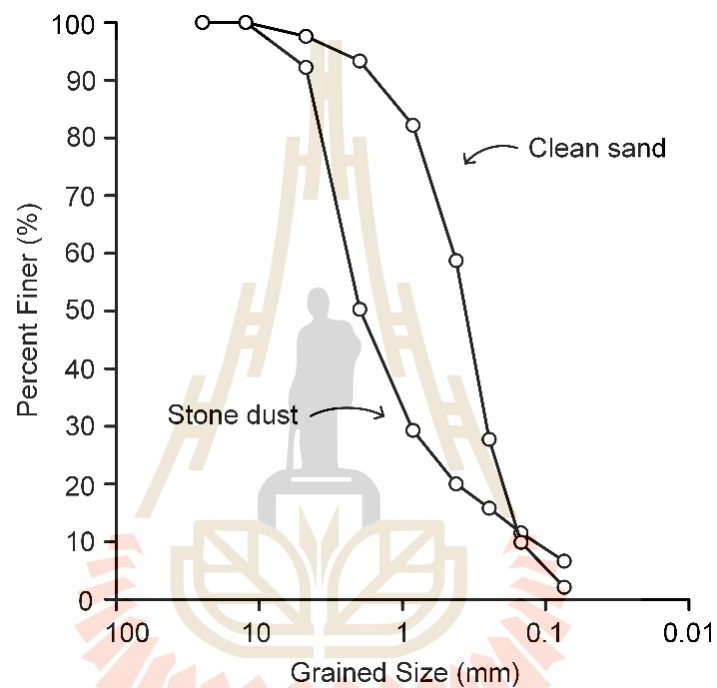
Figure 4.1   Particle size distributions of stone dust and clean sand used in this study.

Table 4.1   Stone dust and clean sand classification based on USCS.

Aggregates	Gravel (%)	Sand (%)	Silt (%)
Stone dust	2.4	95.5	2.1
Clean sand	3.9	95.1	1.0

Table 4.2   Ranges of stone dust and clean sand sizes for stage I separation.

Samples No.	Particles size (mm)	
	From	to
SD-04-10	4.75	2.0
SD-10-20	2.0	0.85
SD-20-40	0.85	0.425
SD-40-60	0.425	0.25
SD-60-100	0.25	0.15
SD-100-200	0.15	0.075
SD-04-200	4.75	0.075
Clean sand	4.75	0.075
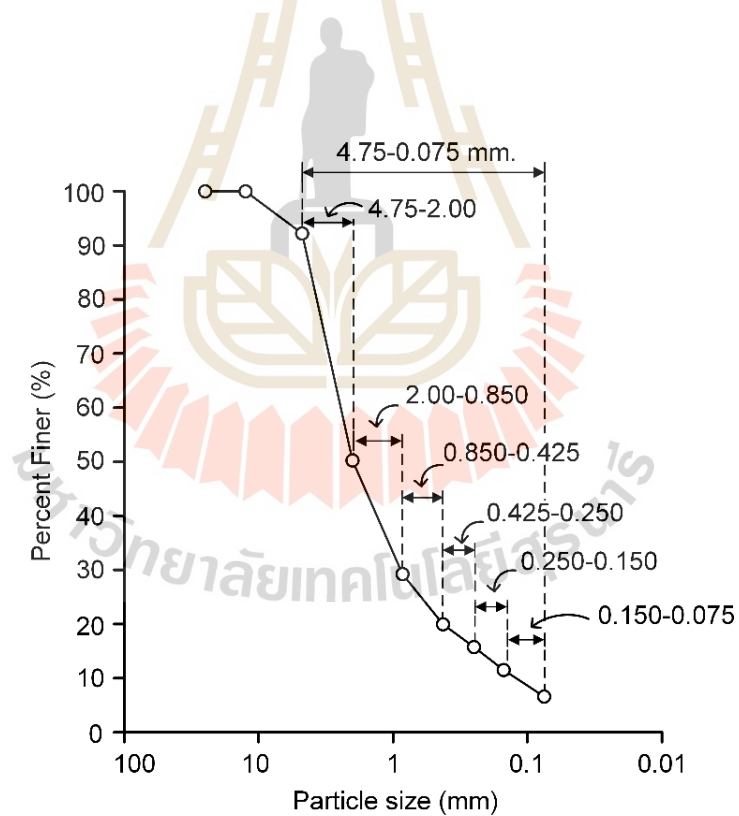
Figure 4.2   Separations of particle size ranges for cement mixtures for stage I testing.

Table 4.3   Ranges of stone dust and clean sand sizes for stage II separation.

Particle size range of separated	Sample no.	Particles size (mm)	
		From	to
Set I	SD-04-60	4.75	0.25
	SD-60-200	0.25	0.075
Set II	SD-04-100	4.75	0.15
	SD-100-200	0.15	0.075
Clean sand	Clean sand	4.75	0.075
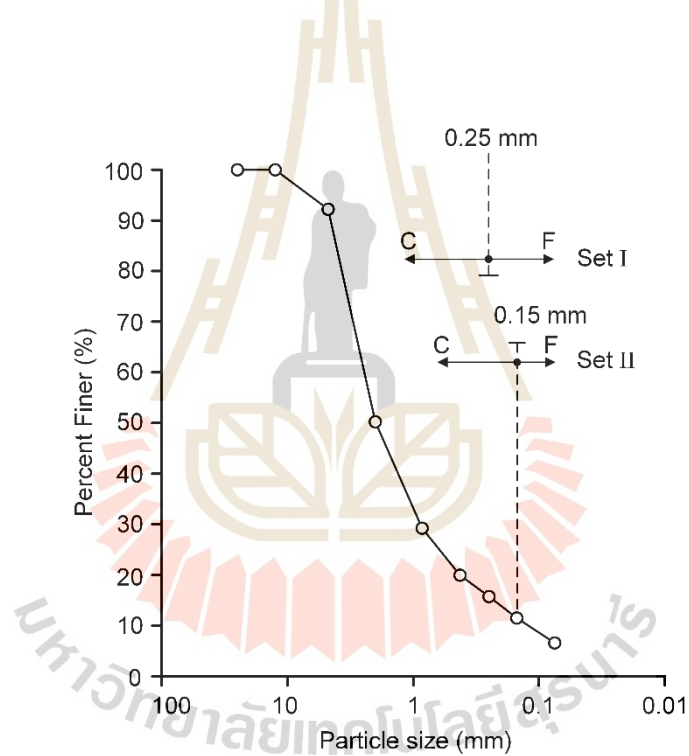
Figure 4.3   Separations of particle size ranges for cement mixtures for stage II testing.

4.2.2   Mixture procedure

To determine the mechanical properties of particle size ranges for cement mixtures. The cement used is Portland cement type I, ratio of the stone dust-cement-water (SD:C) is set as 2:1 with water-cement (W:C) ratio of 1:0.5 by weight, follow the ASTM C39 standard. A cement mixer is used to mix all components and get a consistent slurry (Figure 4.4). The slurry of all mixtures is poured in cement cast (Figure 4.5) with diameter and length of 15 cm and 30 cm. The curing time is 7 days under water. The mixing and pouring into cement cast is in accordance with ASTM C192 standard.

Figure 4.4   Cement mixer to mix all components in mechanical properties test.
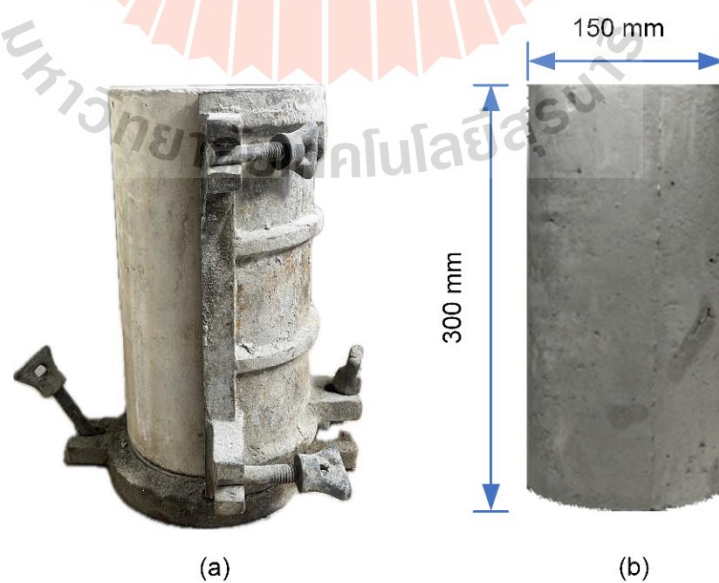
Figure 4.5   Example image of cement cast (a) and cement mixture specimens (b).

4.3   Uniaxial compression tests

4.3.1   Test method

The compressive strengths of stages **I** and **II** specimens are evaluated after a 7-day curing period. This evaluation involved axial loading of the specimens under a constant loading rate of 0.1 MPa/second until failure occurred (Figure 4.6). Both axial and lateral displacements are monitored throughout the testing process. In accordance with ASTM C39 standard practice, compressive strength, elastic modulus, and Poisson's ratio are determined for each specimen. Post-failure observations are conducted, and any noteworthy characteristics are documented for future reference. Tables 4.4 and 4.5 present the dimensions and weights of the specimens employed in the uniaxial compression tests for both stages.
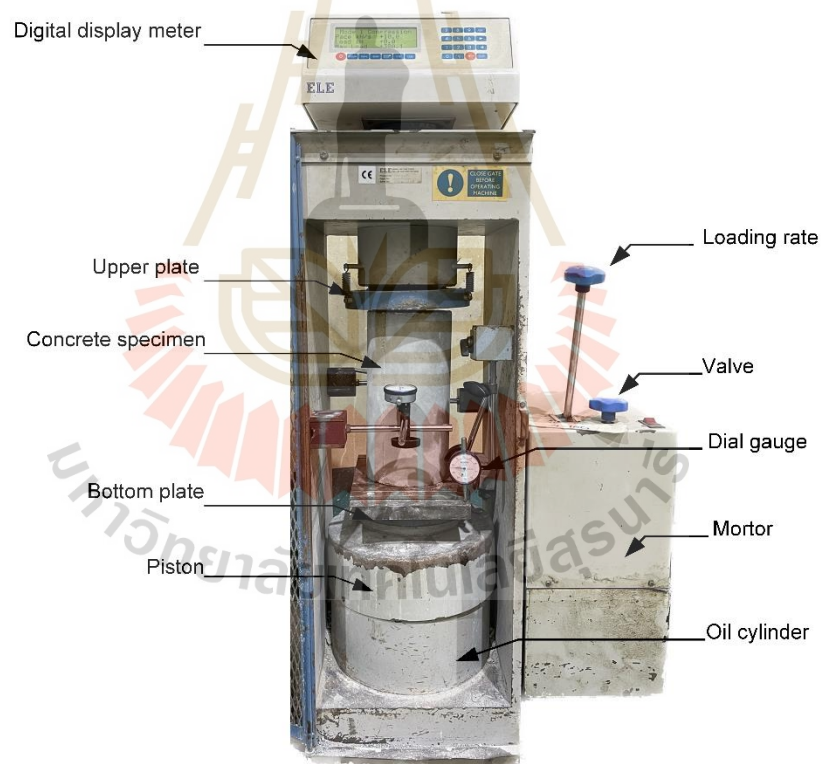
Figure 4.6   Laboratory arrangement for compression testing.

Table 4.4   Stone dust-cement mixtures specimens of stage **I** prepared for compression tests.

Sample No.	Particles size (mm)		Diameter	Length	Weight	L/D	Density
	From	to	(mm)	(mm)	(kg)		(g/cc)
SD-04-10	4.75	2.0	149.6	298.2	11.48	1.99	2.19
SD-10-20	2.0	0.85	149.5	302.6	11.66	2.02	2.20
SD-20-40	0.85	0.425	148.7	297.5	11.44	2.00	2.22
SD-40-60	0.425	0.25	148.7	297.5	11.32	2.00	2.19
SD-60-100	0.25	0.15	148.7	297.5	11.12	2.00	2.15
SD-100-200	0.15	0.075	148.7	297.5	10.60	2.00	2.05
SD-04-200	4.75	0.075	149.6	298.2	11.48	1.99	2.19
Clean sand	4.75	0.075	149.5	302.6	11.66	2.02	2.20

Table 4.5   Stone dust-cement mixtures specimens of stage **II** prepared for compression tests.

Particle size range of separated	Sample no.	Particles size (mm)		Diameter	Length	Weight	L/D	Density
		From	to	(mm)	(mm)	(kg)		(g/cc)
Set **I**	SD-04-60	4.75	0.25	150.0	302.1	12.12	2.01	2.27
	SD-60-200	0.25	0.075	151.5	303.2	11.24	2.00	2.06
Set **II**	SD-04-100	4.75	0.15	152.6	303.7	12.20	1.99	2.20
	SD-100-200	0.15	0.075	150.0	301.2	10.92	2.01	2.05
Clean sand		4.75	0.075	149.6	290.6	10.64	1.94	2.08

4.3.2 Uniaxial compression test results

All post-tested specimens of stage **I** and **II** are shown in Figure 4.7 and 4.8. The stress-strain curves for each size range of stone dust for both stages from initial loading until failure are shown in Figures 4.9 and 4.10. For the test results, it can be seen that the compressive strengths and elastic moduli is higher for particle sizes of 0.85-0.425 mm for stage **I** and particle sizes of 4.75-0.25 mm for stage **II**. They decrease with decreasing particle sizes. The strengths and elastic moduli are higher than those mixed with clean sand (Figures 4.11 and 4.12). The Poisson's ratio tends to be similar for all specimens, suggesting that the particle size ranges do not affect the specimen dilation (Figure 4.13). Mixtures containing finer aggregate particles generally exhibit superior mechanical performance, characterized by increased strength and elastic modulus, compared to mixtures incorporating coarser aggregate particles. This is probably due to limestone with small particle sizes having a bonding higher than those with larger particle sizes. In addition, the small particle size can fill the pores spaces between cement particles in paste better which is known as a filling effect. Thus, the fineness of stone dust has influence on the observed compressive strength values Thongsanitgarn et al. (2011). Porosity is an important factor influencing the behavior of specimens. Studies have demonstrated that lower porosity is directly correlated with enhanced uniaxial compressive strength and Young's modulus (Srikanth and Mishra, 2016; Ghafoori et al., 2016). The test results are summarized of stage **I** and **II** are given in Tables 4.6 and 4.7. All specimens fail under longitudinal mode.

SD-04-10 SD-10-20 SD-20-40 SD-40-60

SD-60-100 SD-100-200 SD-04-200 Clean sand

Figure 4.7   Post-test specimens of stage I for uniaxial compressive strength.

Set I

SD-04-60   SD-60-200

Set II

SD-04-100   SD-100-200

Clean sand

Figure 4.8   Post-test specimens of stage **II** for uniaxial compressive strength.
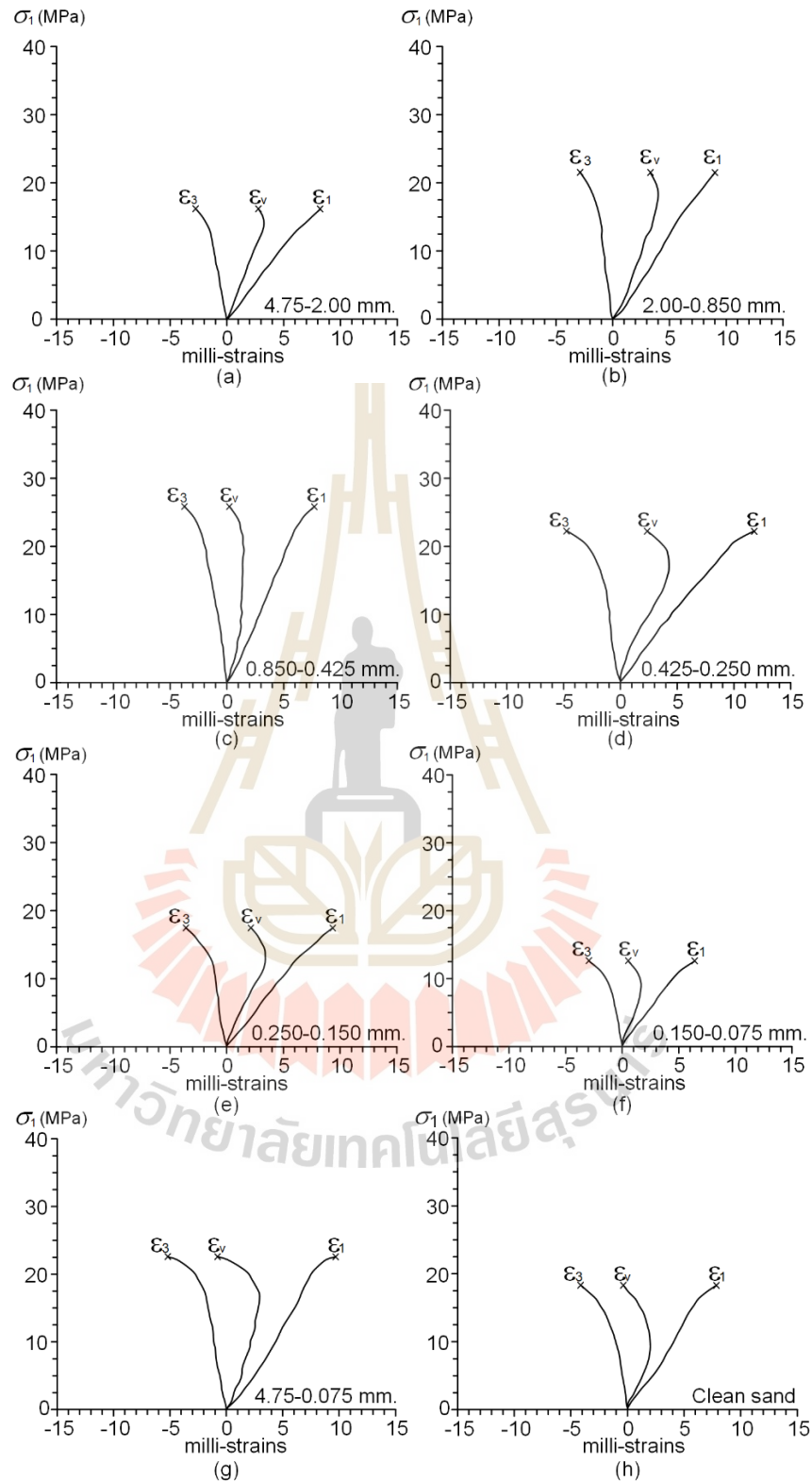
Figure 4.9   Stress-strain curves of stage **I** for size ranges of 4.75-2.0, 2.0-0.85, 0.85-0.425, 0.425-0.25, 0.25-0.15, 0.15-0.075, 4.75-0.075 and clean sand (mm). as shown in (a) thought (h).
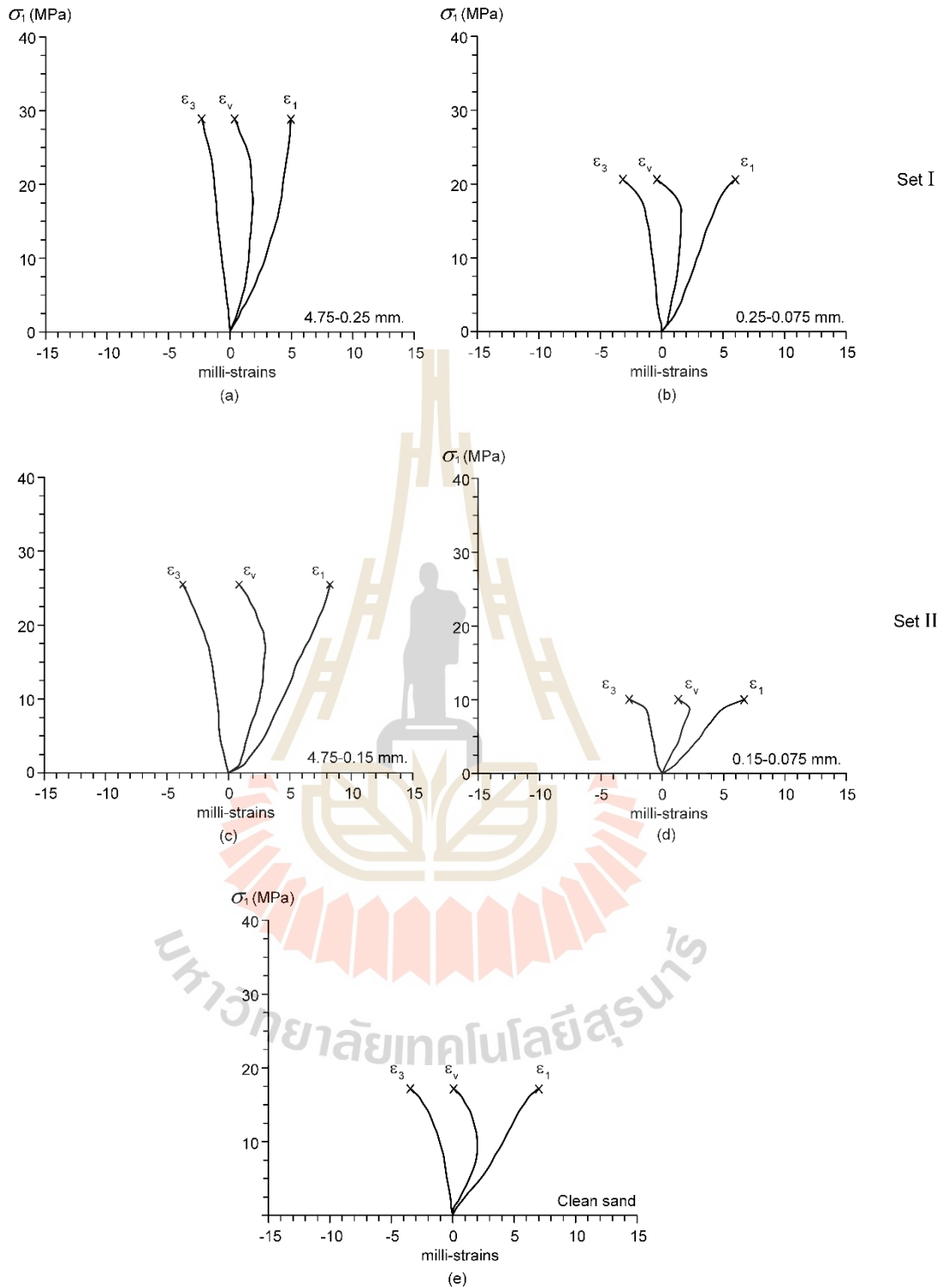
Figure 4.10   Stress-strain curves of stage **II** for size ranges of 4.75-0.25, 0.25-0.075, 4.75-0.15, 0.15-0.075, and clean sand (mm). as shown in (a) thought (e).
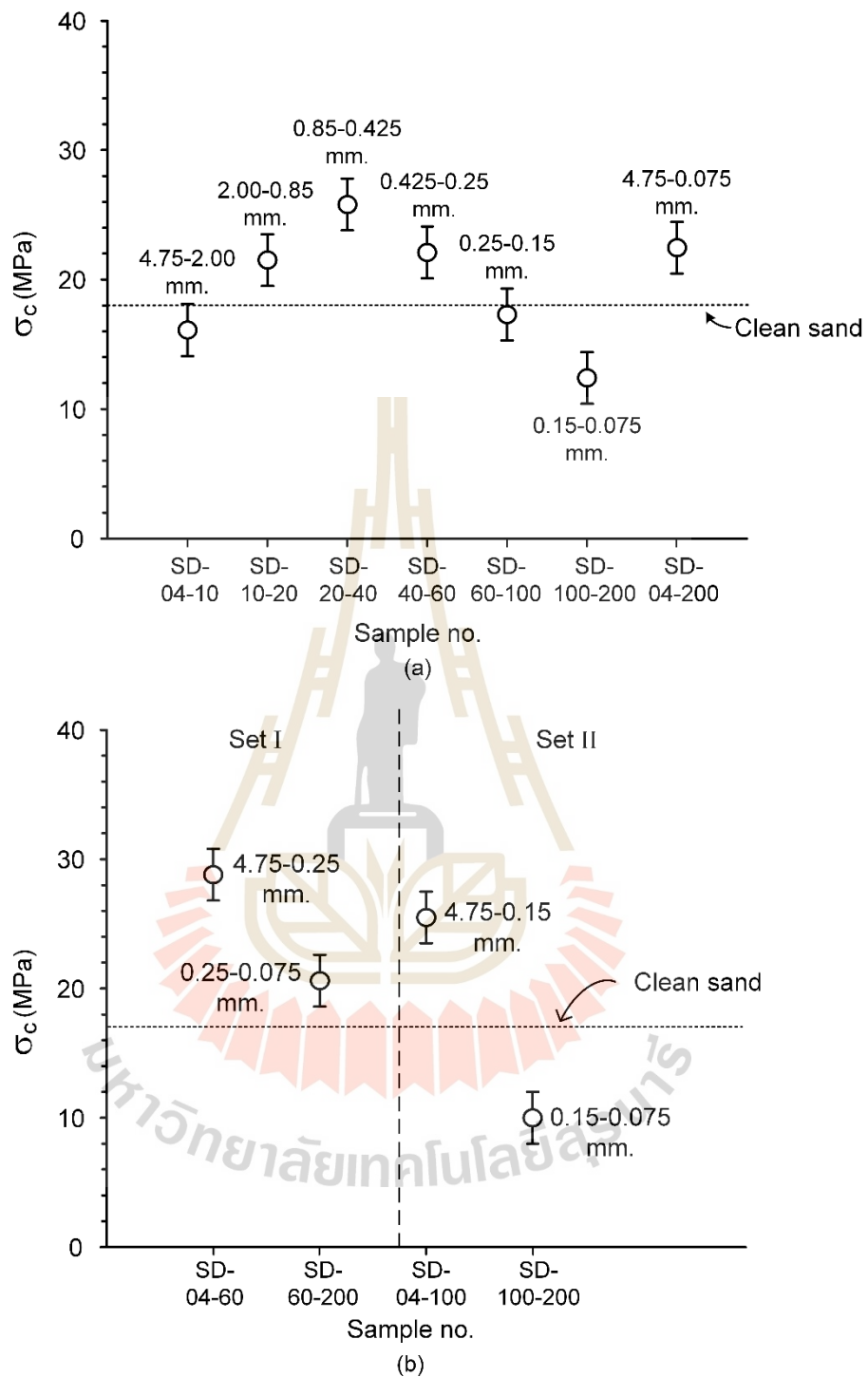
Figure 4.11   Compressive strengths of stone dust mixed with cement of stage **I** (a), and stage **II** (b).
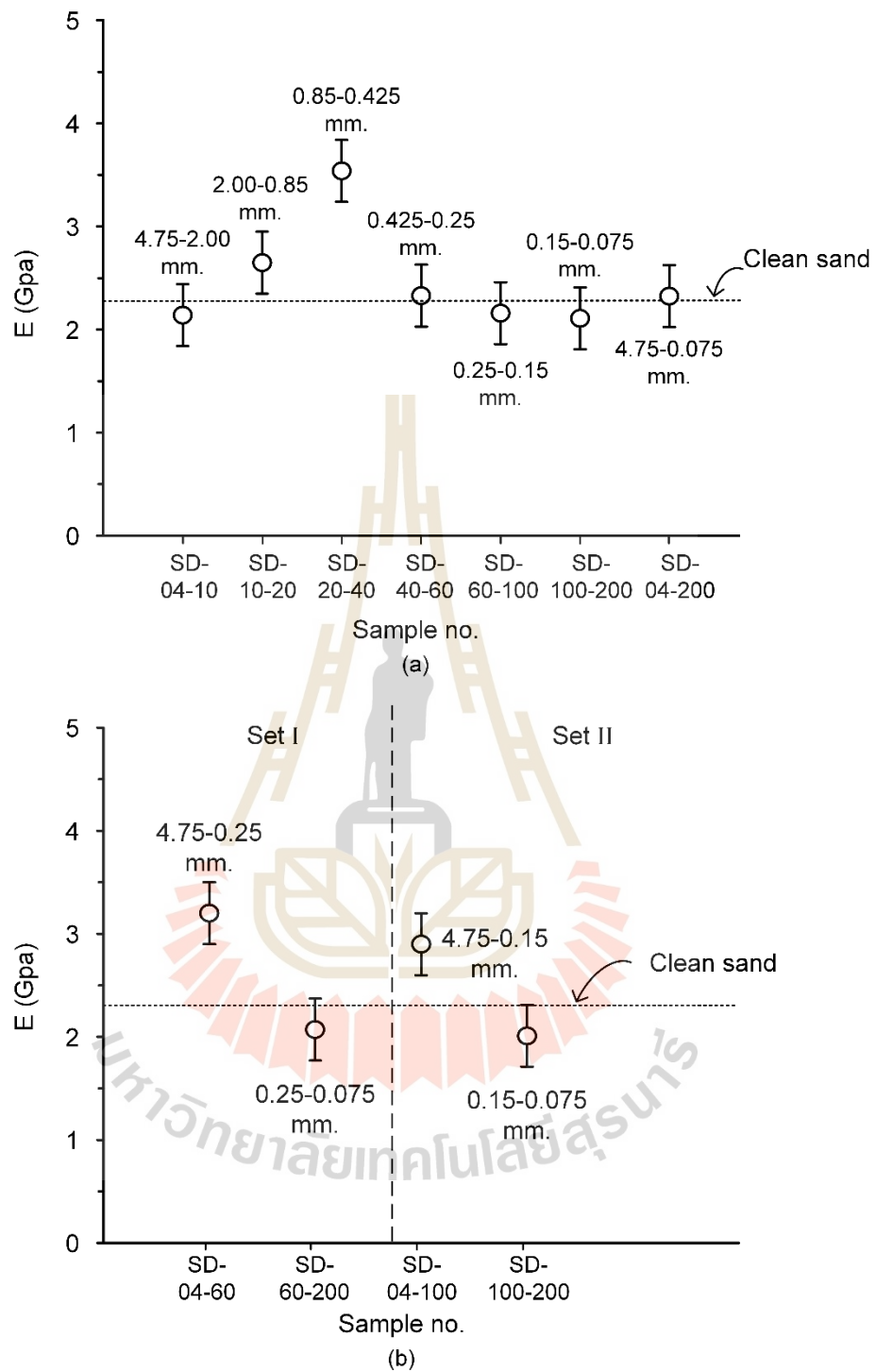
Figure 4.12   Elastic modulus of stone dust mixed with cement of stage **I** (a), and stage **II** (b).
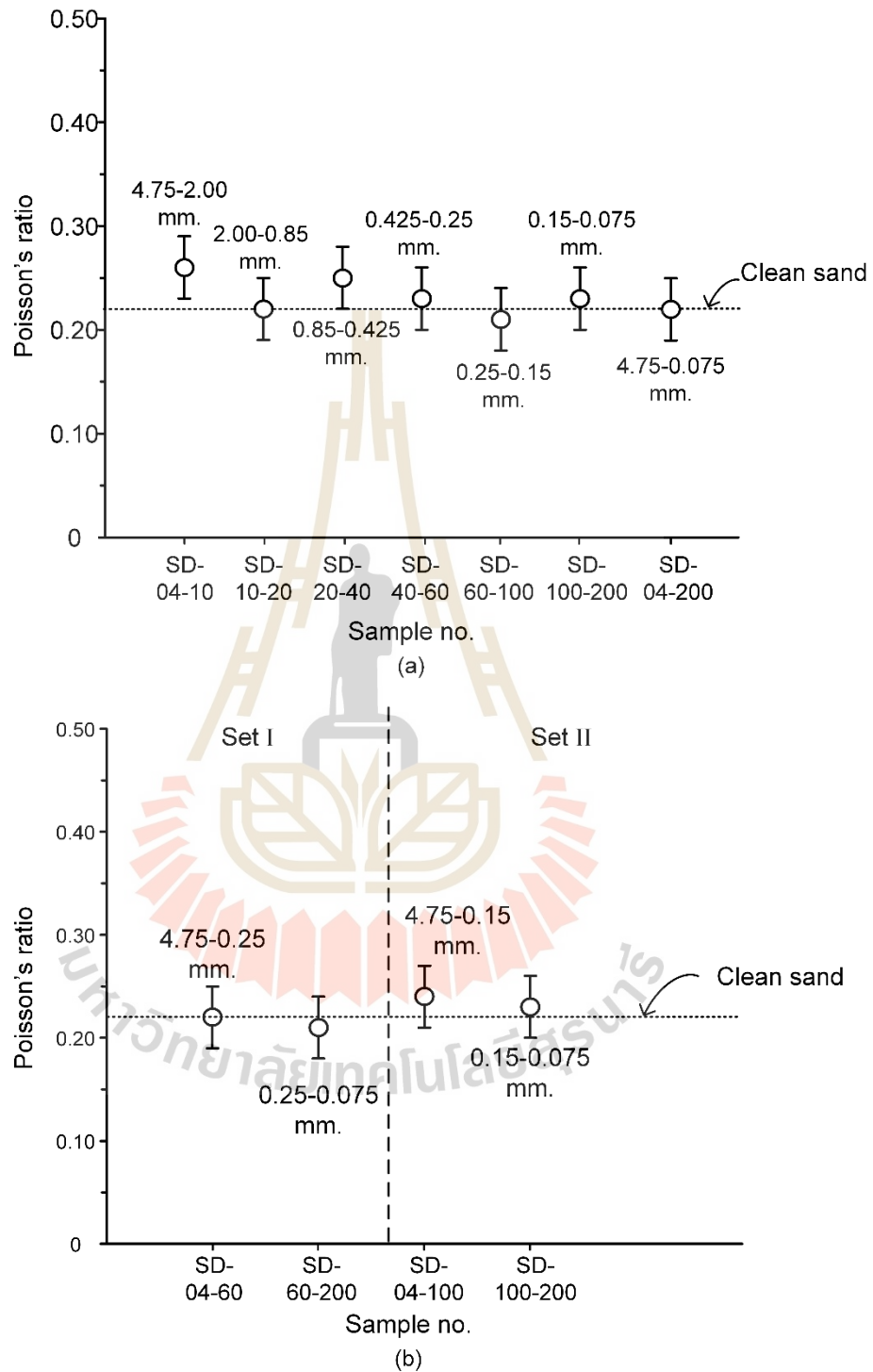
Figure 4.13   Elastic modulus of stone dust mixed with cement of stage I (a), and stage II (b).

Table 4.6   Uniaxial compressive strength test results of stage **I**.

Samples No.	Particles size(mm)		Strength (MPa)	Elastic Modulus (GPa)	Poisson's Ratio
	From	to			
SD-04-10	4.75	2.0	16.1	2.14	0.26
SD-10-20	2.0	0.85	21.5	2.65	0.22
SD-20-40	0.85	0.425	25.8	3.54	0.25
SD-40-60	0.425	0.25	22.1	2.33	0.23
SD-60-100	0.25	0.15	17.3	2.16	0.21
SD-100-200	0.15	0.075	12.4	2.11	0.23
SD-04-200	4.75	0.075	22.4	2.33	0.22
Clean sand	4.75	0.075	18.1	2.28	0.22

Table 4.7   Uniaxial compressive strength test results of stage **II**.

Particle size range of separated	Sample no.	Particles size(mm)		Strength (MPa)	Elastic Modulus (GPa)	Poisson's Ratio
		From	to			
Set **I**	SD-04-60	4.75	0.25	28.8	3.21	0.22
	SD-60-200	0.25	0.075	20.6	2.07	0.21
Set **II**	SD-04-100	4.75	0.15	25.5	2.49	0.21
	SD-100-200	0.15	0.075	10.0	2.01	0.23
Clean sand		4.75	0.075	17.1	2.31	0.22

CHAPTER V
LABORATORY TESTING

5.1   Introduction

This chapter describes geotechnical testing, including methods and results of the compaction, direct shear, and consolidation tests. Particle sizes of less than 0.25 mm (set I) are used here to mix with construction grade bentonite. Compaction tests are performed to obtain the maximum dry density and optimum water content under different mixing ratios. The specimens after compaction are used for the direct shear and consolidation testing.

5.2   Compaction test

5.2.1   Test method

The fine-grained stone dust classified in the previous chapter is mixed with bentonite using percentages of bentonite of 100, 80, 60, and 40% by weight. The mixtures are prepared in stainless steel tray using 2.7 kilograms of the mixture (Figure 5.1). Water is added to the mixture until the desired water content is reached. The components are thoroughly mixed using a spatula to ensure uniform distribution. In accordance with the ASTM D1557-12 (2021) standard method, the mixture is then compacted within the mold using a 10-pound weight dropped and released 27 times per layer for a total of five layers (Figure 5.2).

Figure 5.1   Fine-grained stone dust mixed with bentonite prepared in plastic tray.
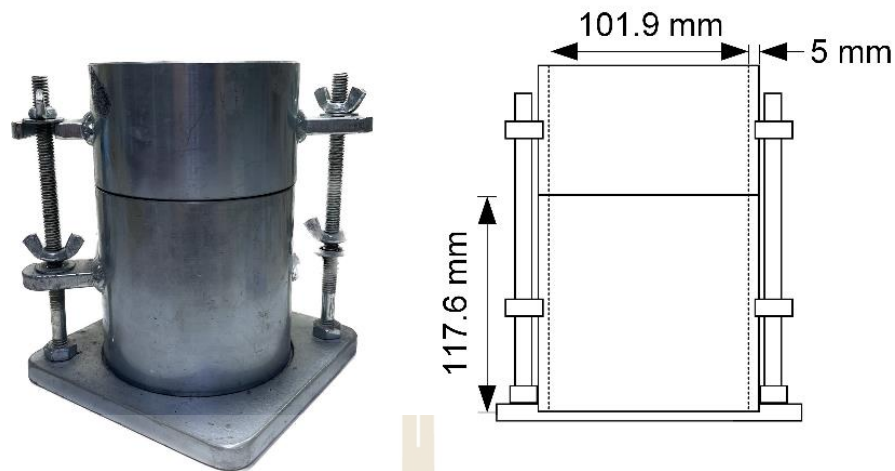
Figure 5.2   Compaction mold based on ASTM D1557-12 (2021) standard method.

5.2.2   Test results

The results show the maximum dry unit weight (ρ_{dry}) as a function of water weight ratios in Figure 5.3. The data reveals a trend of increasing maximum dry density with increasing stone dust ratios. This observation suggests that coarser mixtures achieve higher dry densities compared to finer ones. As water content is introduced, the volume of voids within the mixture increases, leading to a corresponding decrease in density (Figure 5.4). Also show the rise in maximum unit weight with increasing stone dust weight ratios, where the mixtures after compaction have higher unit weight than those before compaction. Figure 5.5 shows trend of optimum water content, which decreases as the bentonite weight ratio increases. A summary of the compaction test results is provided in Table 5.1."
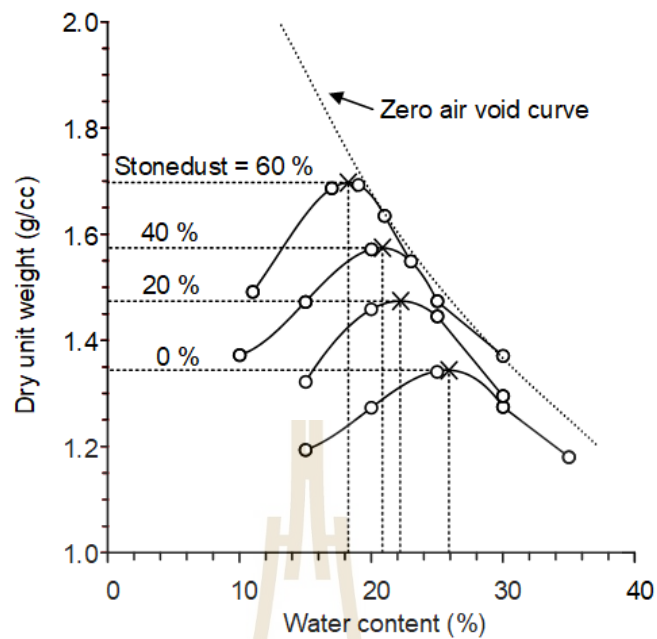
Figure 5.3   Maximum dry unit weight as a function of water content for various stone dust-bentonite mixing rations.
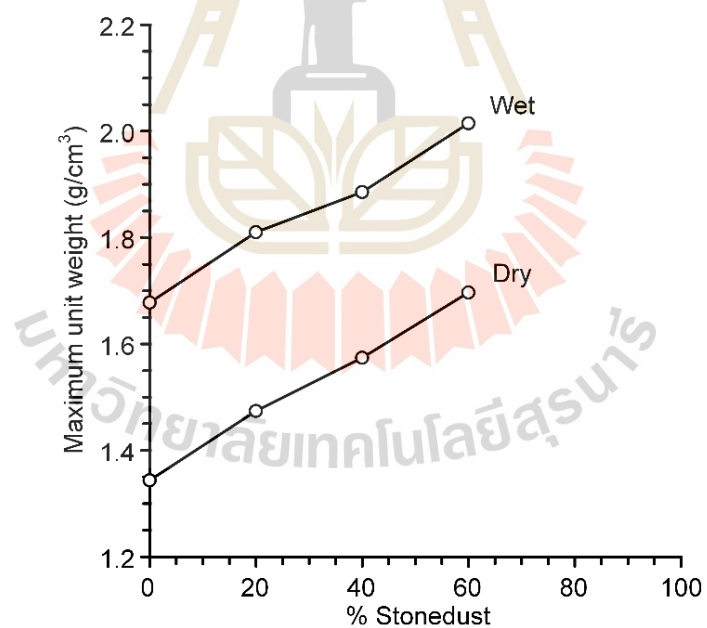
Figure 5.4   Maximum unit weight as a function of fine-grained stone dust-bentonite weight ratio comparing before and after compaction.
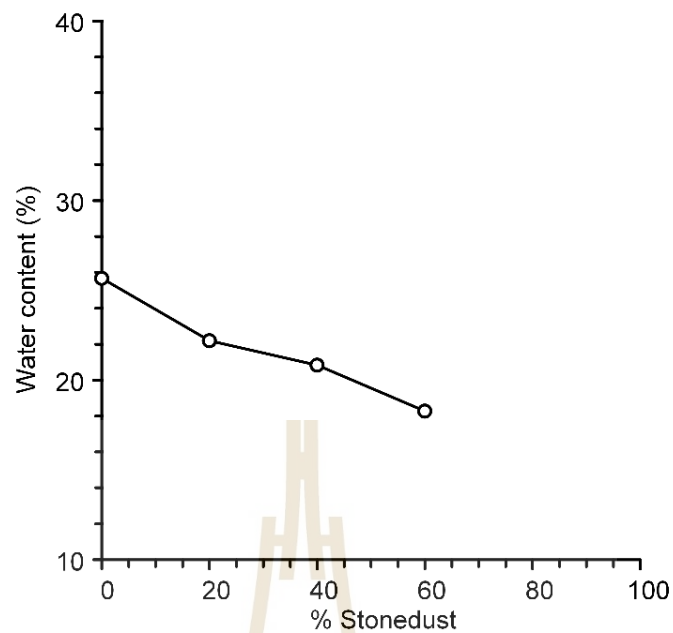
Figure 5.5   Optimum water content as a function of fine-grained stone dust-bentonite weight ratio.

Table 5.1   Compaction test results.

Fine grained stone dust: Bentonite (SD:B)			
Weight ratio (SD:B)	Sample No.	Maximum dry densities (g/cc)	Optimum water contents (%)
0:100	SD-0	1.34	25.67
20:80	SD-20	1.47	22.20
40:60	SD-40	1.57	20.83
60:40	SD-60	1.70	18.27

5.3   Direct Shear test

5.3.1   Test method

A direct shear test is conducted to determine the peak shear strength of the compacted specimens comprised of bentonite mixed with fine-grained stone dust. The compaction process utilizes the optimum water content for each specimen. Following compaction, the specimens are trimmed using a soil trimmer before being placed within a dedicated stainless steel shear box (Figure 5.6). A hydraulic load cell facilitates the application of constant normal stresses in stages of 25 psi, 50 psi, 75 psi,

and 100 psi. Shear stress is then applied, and both the shear displacement and dilation are meticulously recorded at intervals of 0.01 mm.

5.3.2 Test results

The shear stresses in terms of shear displacement are shown in Figure 5.7. The result show trend of increasing shear stresses with increasing shear displacement, particularly evident under high normal stress conditions. Additionally, the figure demonstrates a significant correlation between increasing aggregate particle size and the magnitude of dilatation observed.

Specimens with lower bentonite percentages exhibited greater shear strengths compared to those with higher bentonite content. The relationships between cohesion and friction angle for the various mixtures are shown in Figure 5.9. The data suggests that an increase in the fine-grained stone dust content leads to a decrease in cohesion (c). While a reduction in the bentonite percentage results in an increase in friction angle (ϕ). This trend can potentially be attributed to the enhanced frictional resistance between the grain surfaces within the stone dust mixture.
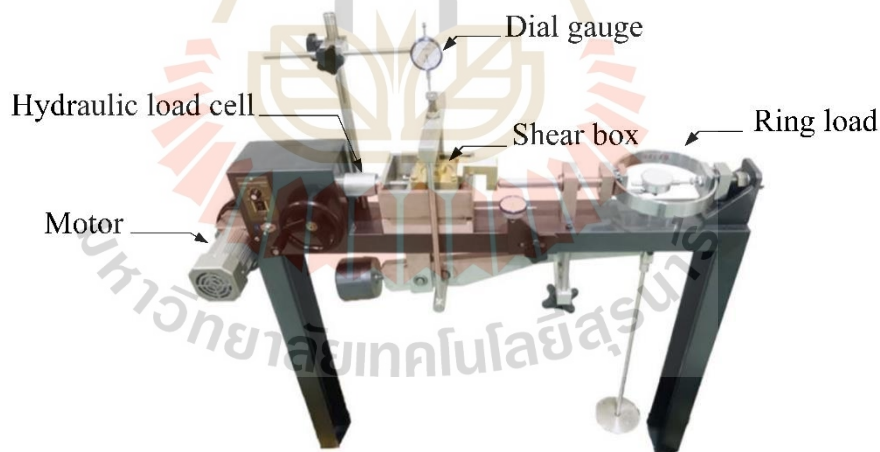
Figure 5.6   Direct shear device of fined-aggregates stone dust-mixed bentonite testing using by direct shear machine.
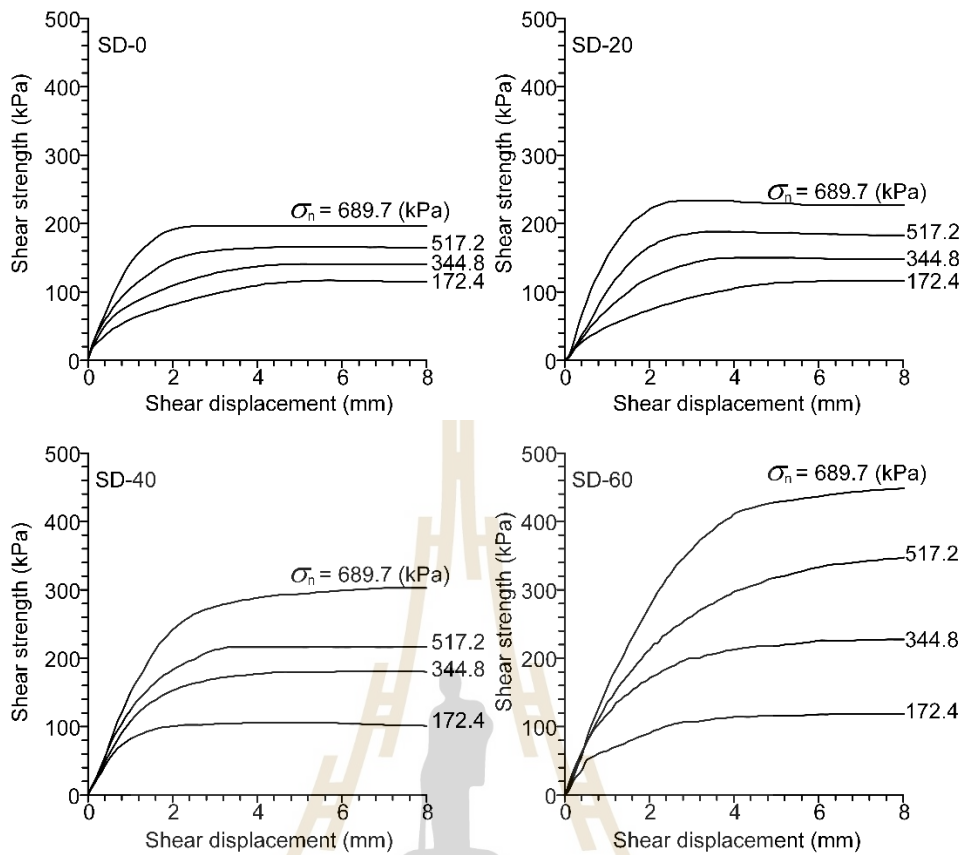
Figure 5.7   Shear stress as a function of shear displacement of fine-grained stone dust-bentonite mixtures.
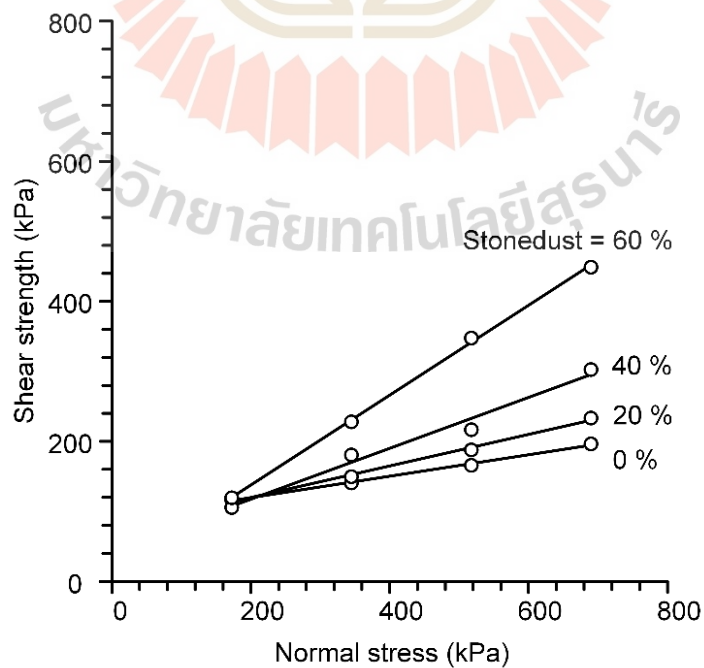
Figure 5.8   Shear strengths as a function normal stress.
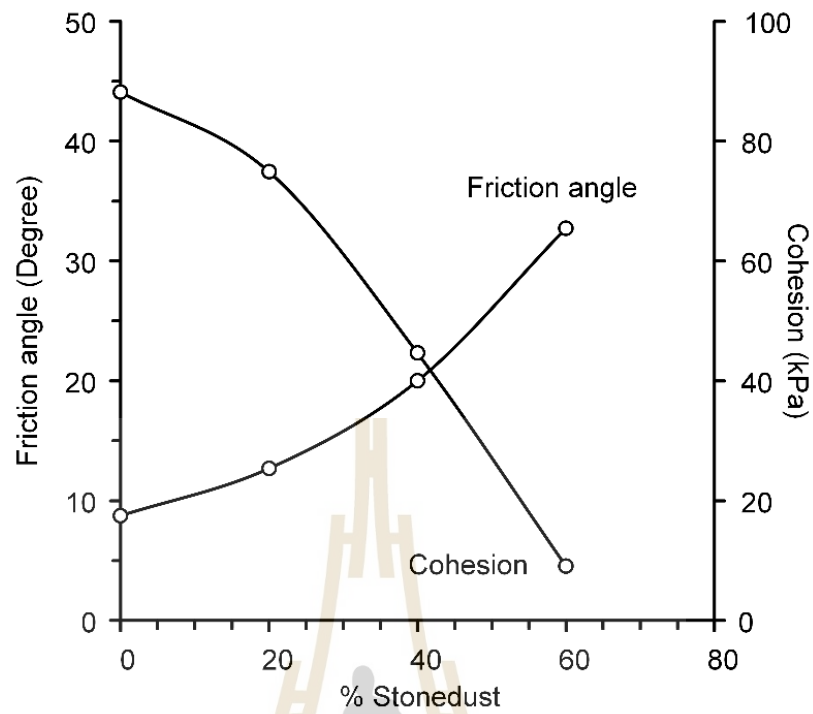
Figure 5.9   The cohesions and friction angles of specimens mixtures for the first
              separator (set I).

Table 5.2   Direct shear test results of fine-grained stone dust-bentonite mixtures
              results.

Fine grained stone dust: Bentonite (SD:B)			
Weight ratio	Sample No.	C (kPa)	Friction angles (ϕ)
0:100	SD-0	88.2	9
20:80	SD-20	74.9	13
40:60	SD-40	44.7	20
60:40	SD-60	9.1	33

5.4 Consolidation test

5.4.1 Test method

Consolidation tests are conducted on the prepared mixtures using their previously determined optimum water content. Constant axial stresses are applied via a hydraulic load cell (Figure 5.10). The applied axial stresses encompassed a range from 10 kPa to 1280 kPa in increments of 10, 20, 40, 80, 160, 320, 640, and 1280 kPa. Each test is maintained for a duration of 10 days under ambient temperature conditions. High-precision gauges are employed to record the axial displacements throughout the testing process.

Figure 5.10   Consolidation testing of fined-aggregates stone dust-mixed bentonite testing using by Soil test pro machine.

5.4.2 Test results

The relationship between the void ratio and the effective stress shows downward trends when increasing percentages of fined grained stone dust. The cumulative pore volume decreases with increasing fined grained stone dust percentage as shown in Figure 5.11. The settlement of fine-grained stone dust-bentonite mixtures decreases when the fined grained stone dust contents increase. This could be the pore filling phenomena, which occurs with addition of bentonite particles to fine grained stone dust. The bentonite particles can penetrate inside the void spaces created by the fined grained stone dust, which stiffens the specimens matrix.
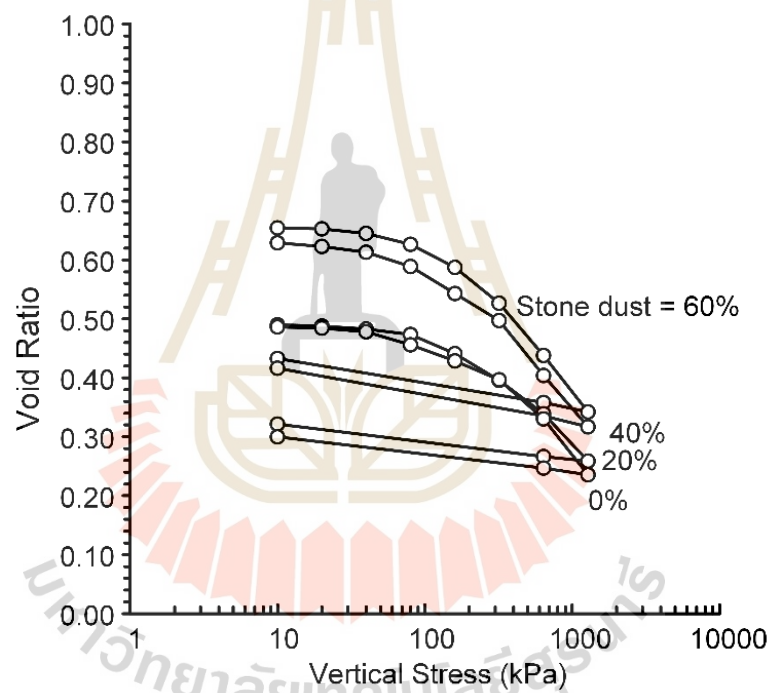
Figure 5.11   Void ratio as a function of effective stress of fine-grained stone dust-bentonite mixtures.

5.5   Swelling test

5.5.1   Swelling tests under different bentonite weight ratios

5.5.1.1 Test method

This study explores the influence of varying weight ratios between fine-grained stone dust and bentonite. The weight ratios studied include 0:100, 20:80, 40:60, and 60:40. Each sample is compacted within a mold in five layers, receiving a total of 27 compaction cycles. Following compaction, the top surface is carefully trimmed to ensure a smooth finish. A porous brass disc is then placed on top of the sample (Figure 5.12). Subsequently, the sample is submerged underwater for testing. During the initial 30 minutes of the test, readings are recorded at one-minute intervals. Following this initial period, the reading frequency gradually increased to hourly intervals. The swelling test method employed adheres to the ASTM D4546-08 standard practice.

5.5.1.2 Test results

Swelling ratio for various bentonite weight ratios are shown in Figure 5.13. The results indicated that the maximum swelling ratio increases with increasing bentonite weight ratio. This is because bentonite characteristically swells when contacts with water. Underwater the swelling increases rapidly within the 6 days, except for the samples with stone dust ratio of 0:100 and 20:80. They fluctuate until 10 days and tend to remain constant for all weight ratios after 30 days under water.

Figure 5.12   Swelling test setup in compaction mold.
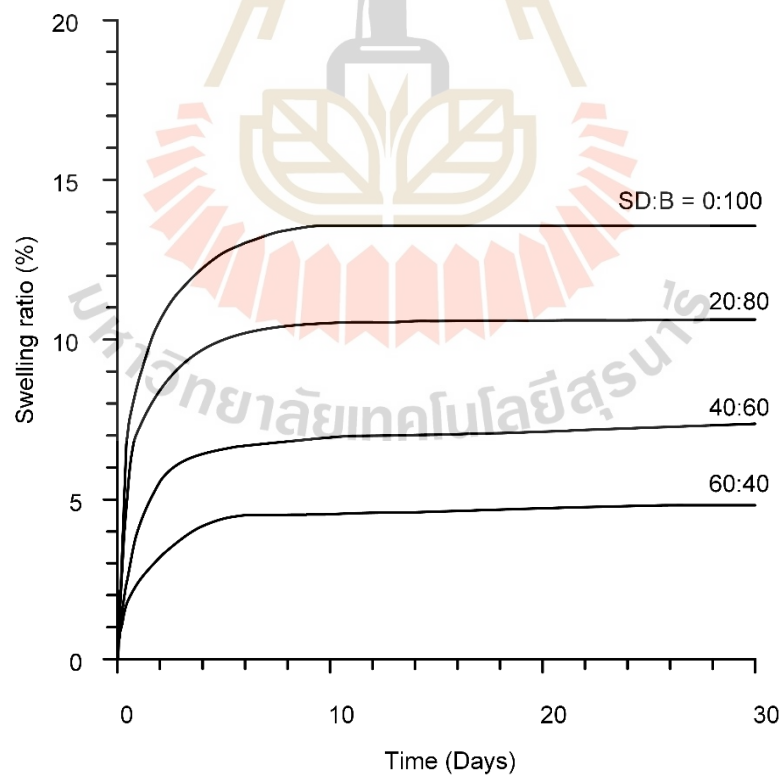
Figure 5.13   Swelling ratio as a function of time.

5.5.2 Swelling test under different constant loads

5.5.2.1 Test method

Specimens prepared with varying bentonite weight ratios are conducted under static loading conditions. Specimens are subjected to constant vertical loads of 2, 4, and 6 kilograms. In accordance with ASTM D4546-08, a consistent supply of water is maintained for the specimens throughout the 15-day testing period. The vertical swelling deformation is monitored at one-minute intervals during the initial 30 minutes of the test. Thereafter, the reading frequency gradually increased to hourly intervals.

5.5.2.2 Test results

The swelling ratios as a function of time under 2, 4 and 6 kg loading are shown in Figure 5.14. Figure 5.15 show the swelling behavior of the compacted fine-grained stone dust-bentonite mixtures under various constant loading conditions. The results suggest an inverse relationship between swelling ratio and applied static load. This observation can potentially be attributed to the influence of vertical stress on the internal structures of the compacted specimens. An increase in vertical stress may lead to a compaction of the spaces between aggregates, thereby reducing the potential for swelling strain.
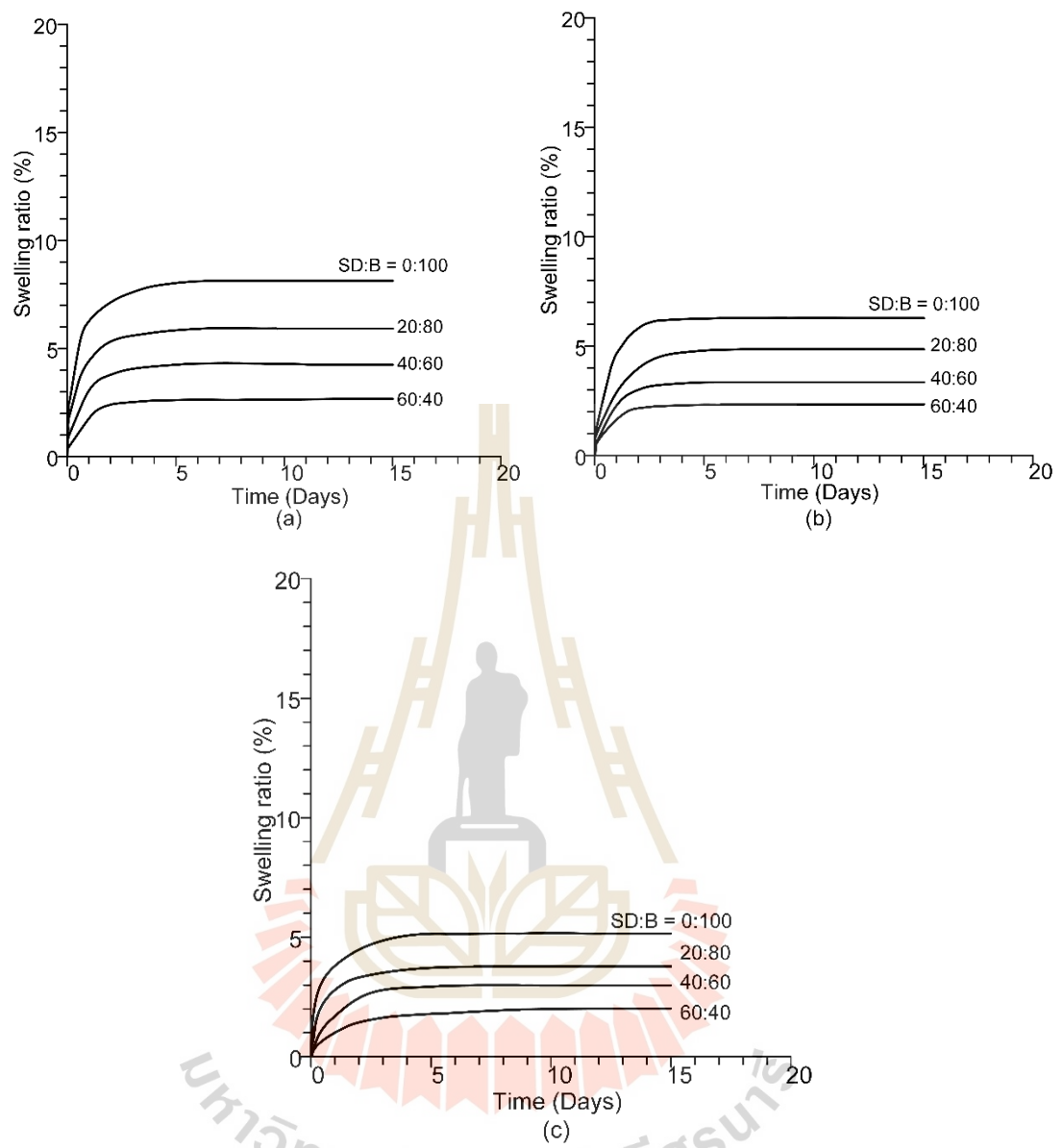
Figure 5.14 Swelling ratios of fined grained stone dust-bentonite mixtures as a function of time under loads of 2 kg (a), 4 kg (b) and 6 kg (c).
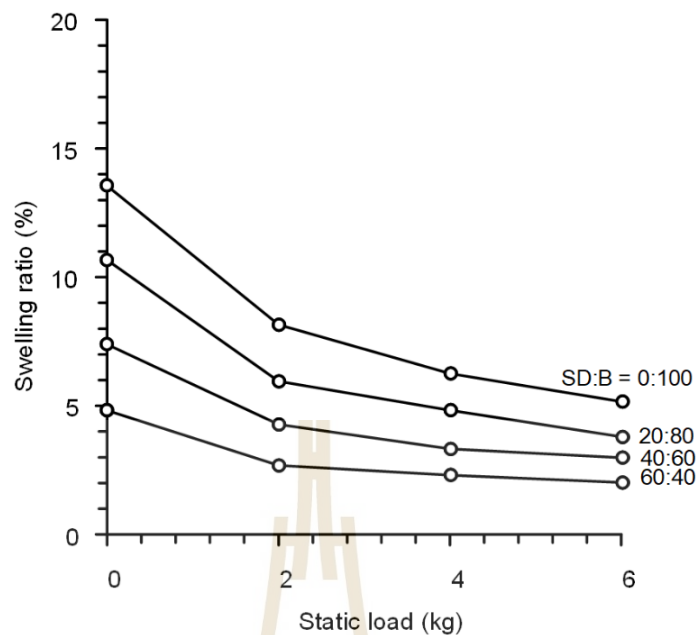
Figure 5.15 Swelling ratios of fined grained stone dust-bentonite mixtures as a function of static load.

5.6 Permeability test under falling head

The primary objective of the falling head tests is to determine the permeability of stone dust. The test uses stone dust particles smaller than 0.25 mm, categorized into three sizes: 0.25 mm, 0.15 mm, and 0.075 mm.

5.6.1 Test method

The hydraulic conductivity of the specimens is determined using a permeability test apparatus. The test setup employs standpipes with diameters of 6 mm, 10 mm, and 13 mm to facilitate the calculation of the internal cross-sectional area. Water from the standpipe is permitted to flow through the sample contained within a mold having a diameter of 101 mm and a length of 122 mm. To minimize potential water leakage along the sides of the cell, a thin layer of grease is applied to the inner surfaces of the mold. In order to reduce the presence of air voids, the test material is thoroughly compacted using a rammer device in three layers of approximately equal heights. Two filter papers are placed at the interface between the upper and lower portions of the tested material. During the testing process, the initial water level within the standpipe is designated as h_1. The water is then allowed to flow freely, and the time taken for the water level in the standpipe to reach h2 is

measured. It's important to note that the total head difference, which drives the water flow through the soil sample, varies throughout the test from h_1 to h_2 (Figure 5.16). The collected data is subsequently employed to calculate the hydraulic conductivity value (k), which can be determined using Darcy's Law as follows:

$$k=2.3 \frac{a_m L}{At} \log \left(\frac{h_1}{h_2}\right)$$ (5.1)

where a is internal cross-sectional area of standpipe, L is length of soil sample, or the distance water flows through the soil mass during the experiment, A is sample area, in the direction perpendicular to water flow, t is time for the water in the standpipe to decrease from level h_1 (initial water level) to level h_2 (final water level) at time t, h_1 represents the energy difference driving water flow through the sample at the start of the test timer, h_2 represents the energy difference causing water to flow through the sample at the end of the test at time t.
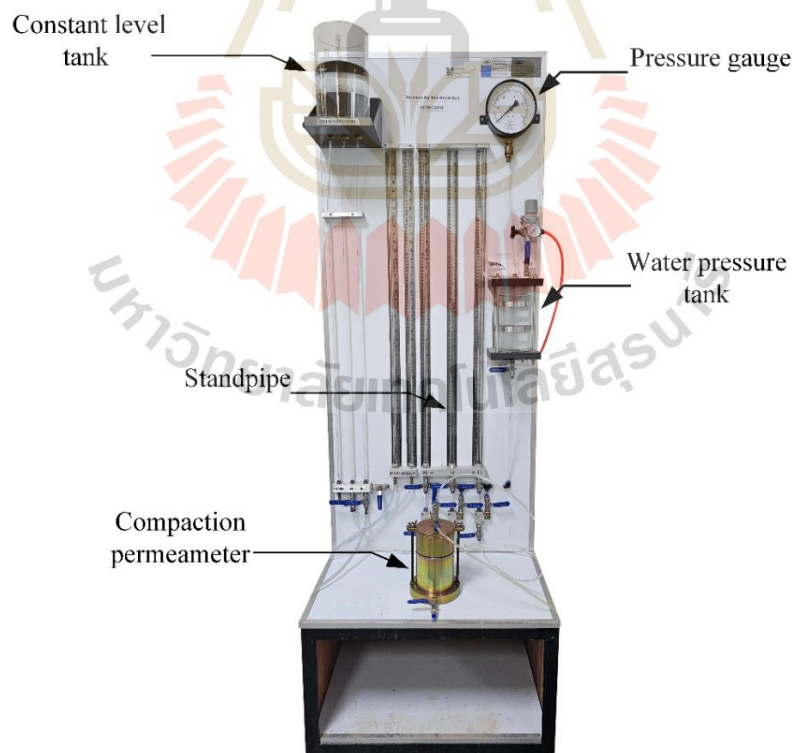
Figure 5.16 Permeability test apparatus of stone dust under falling head.

5.6.3 Test results

The results show that the grain size of 0.25 mm exhibits the highest flow rate, with a permeability coefficient (k) of 7.19×10^{-4} cm/s. This is significantly higher than the k values for the other grain sizes. In contrast, the grain size of 0.075 mm has the slowest flow rate, with a k value of 2.32×10^{-4} cm/s. This finding is consistent with the theoretical expectation that finer materials with smaller pores have lower permeability. All test results are shown in Table. 5.3 and Figure 5.17

An analysis of the results demonstrated a clear correlation between grain size and permeability. As the grain size increases from 0.075 mm to 0.25 mm, the permeability coefficient (k) also increases significantly. This trend is consistent with the theoretical understanding of permeability, where larger pores facilitate faster flow of fluids. However, when grain size of more than 0.25 mm, the increase in permeability is less pronounced.
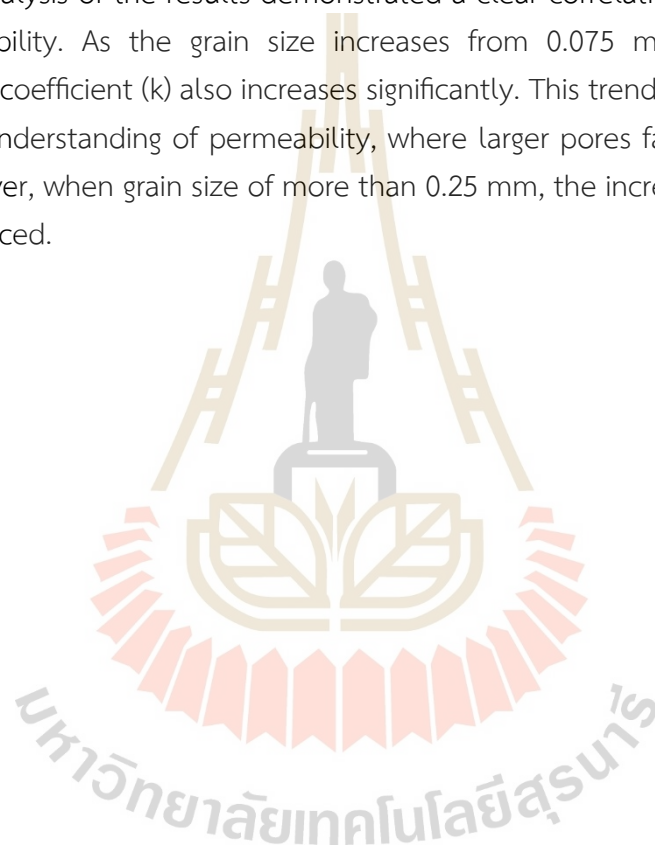
Table 5.3   Test results of permeability under falling head of each particle sizes.

	Grains size 0.25 mm							
Test No.	Manometers		Head, h (cm)	t (s)	A_m (cm^2)	k_t (cm/s)	η_t/η_{20}	k_{20} (cm/s)
	h_1	h_2						
1	80.0	70.0	10.0	18.0	0.28	3.15E-04	0.906	2.86×10^{-4}
2	80.0	70.0	10.0	46.0	0.79	3.43E-04	0.906	3.11×10^{-4}
3	30.0	20.0	10.0	54.0	1.33	1.50E-03	0.906	1.36×10^{-3}
Average Coefficient of Permeability, k_t is 7.19×10^{-4} cm/sec								
Average Coefficient of Permeability, k_{20} is 6.51×10^{-4} cm/sec								
	Grains size 0.15 mm							
Test No.	Manometers		Head, h (cm)	t (s)	A_m (cm^2)	k_t (cm/s)	η_t/η_{20}	k_{20} (cm/s)
	h_1	h_2						
1	50.0	40.0	10.0	47	0.28	2.02×10^{-4}	0.906	1.83×10^{-4}
2	50.0	40.0	10.0	90	0.79	2.93×10^{-4}	0.906	2.65×10^{-4}
3	50.0	40.0	10.0	144	1.33	3.09×10^{-4}	0.906	2.80×10^{-4}
Average Coefficient of Permeability, k_t is 2.68×10^{-4} cm/sec								
Average Coefficient of Permeability, k_{20} is 2.43×10^{-4} cm/sec								
	Grains size 0.075 mm							
Test No.	Manometers		Head, h (cm)	t (s)	A_m (cm^2)	k_t (cm/s)	η_t/η_{20}	k_{20} (cm/s)
	h_1	h_2						
1	50.0	40.0	10.0	72	0.28	1.32×10^{-4}	0.906	1.19×10^{-4}
2	50.0	40.0	10.0	120	0.79	2.20×10^{-4}	0.906	1.99×10^{-4}
3	45.0	35.0	10.0	146	1.33	3.44×10^{-4}	0.906	3.11×10^{-4}
Average Coefficient of Permeability, k_t is 2.32×10^{-4} cm/sec								
Average Coefficient of Permeability, k_{20} is 2.10×10^{-4} cm/sec								
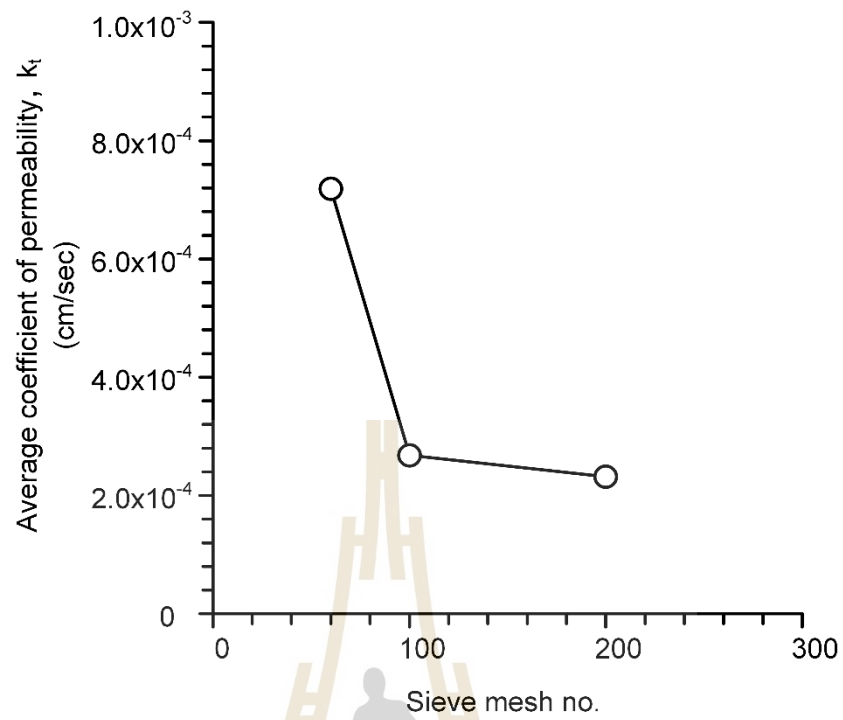
Figure 5.17 Average coefficient of permeability of each sieve mesh no.

CHAPTER VI

DISCUSSIONS, CONCLUSIONS AND RECOMMENDATIONS FOR FUTURE STUDIES

7.1   Discussions

This study determines the potential application of stone dust used for cement and bentonite mixtures. The stone dust for specific size range is mixed with cement to determine the mechanical properties of each mixture. The cement mixtures are divided into two stages. The ranges of stone dust sizes for stage I are 4.75, 2.00, 0.85, 0.425, 0.25, 0.15 and 0.075-mm. Results from stage I testing reveals the detail of the effect of aggregate sizes on the mixture strength. In stage II the stone dust is separated into coarse and fine particles, where only one separator is selected which can be installed between the rock crusher and the stockpile. Two sets of size separations are selected. Set I, particles within the ranges of 4.75-0.25 mm are considered coarse, while those within the range of 0.25-0.075 mm are classified as fine. Set II, particles sized 4.75-0.15 mm are considered coarse, and those within the range of 0.15-0.075 mm are classified as fine. The coarse particles are used for cement mixture, while the fine particles are used for the bentonite mixture.

From the test results of stage I, it can be seen that the compressive strengths are highest for particle sizes of 0.85-0.425 mm and decrease with decreasing particle sizes. The mixture with particle size larger than 0.85 mm tend to show low strength. This is probably due to limestone with small particle sizes has a bonding higher than those with larger particle sizes. This agrees with the test results obtained by Prokopski et al. (2020) that a high concentration of fine grains in a sample may affect its strength.

The compressive strengths and elastic modulus for stage **II**, for cement mixtures show that the coarse particles from set **I** (4.75-0.25 mm) have greater strength as compared to those from set **II** (4.75-0.15 mm). This is supported the results obtained elsewhere (Yalley and Sam, 2018). This is because concrete with higher fine content absorbs more water during hydration leading to the decrease of its strength. As a result, the separation in set **I** is suitable for substituting clean sand. It is supported by the test results obtained from this study that the strength of concrete rises from 17.1 MPa when mixed with clean sand to 28.8 MPa when mixed with coarse particle from set **I**. Only the fine particles from set **I** (0.25-0.075 mm) are therefore considered for the bentonite mixture.

The small particles can fill the pore spaces between cement particles in the paste better than the larger ones which is known as filling effect. The fineness of stone dust has influence on the observed compressive strength values (Cai et al., 2020; Thongsanitgarn et al., 2011). Porosity is an important factor that affects the behavior of specimens, lower porosity leading to greater uniaxial compressive strength and Young's modulus (Srikanth and Mishra, 2016; Ghafoori et al., 2016). A smaller grain size might affect however the strength of specimen. This is supported by the test results obtained by Prokopski et al. (2020) that small particles usually have finer particle size distribution compared to coarse ones. The portion of cement is replaced by stone dust, resulting in a more densely packed mineral concrete component and reduced porosity of the concrete, thus increasing the strength of specimen.

Compaction, direct shear, consolidation, and swelling tests are conducted on mixtures of bentonite and fined stone dust to obtain the optimal ratio. The test results show that the increase of the stone dust weight ratio increases the dry unit weight and decreases the optimum water content. This agrees reasonably well with the test results obtained by Bilal and Ahmad (2020), Thanh Duong and Van Hao (2020), and Pastor et al. (2019). The mixtures containing 60% stone dust exhibit the highest shear strength and friction angle, while yielding the lowest cohesion, settlement, and swelling behavior. This is attributed to the effective filling of small void spaces by the fine particles, resulting in an increase of shear strength. Lower bentonite contents contribute to a reduction of swell capacity. A mixture of 40% bentonite and 60% stone dust may be suitable because it shows the highest maximum dry unit weight, shear strength, and can decrease the cost of the bentonite materials. As suggested by

Johannesson and Nilsson (2006), Borgesson, Johannesson, and Gunnarsson (2003), and Butcher (1993) that for effective compaction the bentonite weight ratio for the mixtures should not be less than 30%. This is primarily to prevent bridging and voids occurring between aggregates particles.

The permeability test results agree with the findings of Hazen (1892), who suggests that the relationship between grain size and permeability becomes less linear for larger grain sizes. The results coincides with previous studies on the relationship between grain size and permeability. For instance, Cabalar and Akbulut (2014), find that permeability increases with increasing grain size for sand samples, with a similar trend observed in this experiment. Additionally, Lopik, Zazai, Hartog, and Schotting (2019) report a nonlinear relationship between grain size and permeability for gravel materials, which is similar to the observation from this study for larger grain sizes of greater than 0.25 mm.

7.2   Conclusions

Conclusions drawn from this study can be summarized as follows.

1)   The compressive strengths and elastic modulus results for cement mixtures show that the coarse particles from set I (4.75-0.25 mm) have greater strength as compared to those from set II (4.75-0.15 mm).

2)   Coarse particles (4.75-0.25 mm) from set I can be used to substitute clean sand for cement mixtures.

3)   Fine particles from set I (0.25-0.075 mm) help reduce the proportion of bentonite material in mechanical and hydraulic work applications.

4)   Fine particles affect concrete strength, they should be used in an optimized ratio to maintain maximum strength.

5)   The increase of fine stone dust (0.25-0.075 mm) weight ratio increases the dry unit weight and decreases the optimum water content.

6)   The mixtures containing 60% stone dust exhibit the highest shear strength and friction angle, while displaying the lowest cohesion, settlement, and swelling behavior. This is due to the filling of small void spaces by the fine particles.

7)   Higher stone dust contents contribute to a reduction of swell capacity.

8)   A mixture of 40% bentonite and 60% stone dust is suitable because it shows the highest maximum dry unit weight, shear strengths.

9)   An effective level of compaction requires a bentonite weight ratio for the mixtures of at least 30%. This is primarily to prevent bridging and voids occurring between aggregate particles.

7.3   Recommendations for future studies

The recommendations for future studies are as follows:

1)   The effects of repeated loading cycles (fatigue) should be investigated to determine their relationship with the physical and mechanical properties of cement and bentonite mixtures for long-term performance evaluation.

2)   Permeability testing should be employed to create mixtures with varying bentonite content and aggregate size.

3)   Further testing is desirable for a diverse range of aggregate types and particle sizes.

4)   The effect of roundness and sphericity of stone dust particles should be studied.

REFERENCE

Akbulut, N., Wiszniewski, M., & Cabalar, A. F. (2015) Influences of grain shape and size distribution on permeability. *2015*, 1451-1454.

Ali, S. M., & Saikrishnamacharyulu, I. (2021). Study of mechanical properties of concrete incorporated with crushed stone sand. *Engineering Research & Technology, 10*(4), 147-152.

American Society for Testing and Materials. (2004). *Annual Book of ASTM Standards: Standard Test Methods for One-Dimensional Consolidation Properties of Soils Using Incremental Loading* (Vol. 04.08). West Conshohocken, PA: ASTM International.

American Society for Testing and Materials. (2006). *Annual Book of ASTM Standards: Standard Practice for Description and Identification of Soils (Visual-Manual Procedure)* (Vol. 04.08). West Conshohocken, PA: ASTM International.

American Society for Testing and Materials. (2012). *Annual Book of ASTM Standards: Standard Specification for Portland Cement* (Vol. 04.01). West Conshohocken, PA: ASTM International.

American Society for Testing and Materials. (2014). *Annual Book of ASTM Standards: Standard Test Method for Direct Shear Test of Soils Under Consolidated Drained Conditions* (Vol. 04.08). West Conshohocken, PA: ASTM International.

American Society for Testing and Materials. (2015). *Annual Book of ASTM Standards: Standard Test Method for Sieve Analysis of Fine and Coarse Aggregates* (Vol. 04.02). West Conshohocken, PA: ASTM International.

American Society for Testing and Materials. (2015). *Annual Book of ASTM Standards: Standard Practice for Making and Curing Concrete Test Specimens in the Laboratory* (Vol. 04.02). West Conshohocken, PA: ASTM International.

American Society for Testing and Materials. (2019). *Annual Book of ASTM Standards: Standard Test Method for Determining the X-Ray Elastic Constants for Use in the Measurement of Residual Stress Using X-Ray Diffraction Techniques*

(Vol. 04.01). West Conshohocken, PA: ASTM International.American Society for Testing and Materials. (2021). *Annual Book of ASTM Standards: standard Test Methods for Laboratory Compaction Characteristics of Soil Using Modified Effort (56,000 ft-lbf/ft3 (2,700 kN-m/m3))* (Vol. 04.08). West Conshohocken, PA: ASTM International.

American Society for Testing and Materials. (2021). *Annual Book of ASTM Standards: Standard Test Methods for One-Dimensional Swell or Collapse of Cohesive Soils* (Vol. 04.08). West Conshohocken, PA: ASTM International.

American Society for Testing and Materials. (2022). *Annual Book of ASTM Standards: Standard Test Methods for Measurement of Hydraulic Conductivity of Coarse-Grained Soils* (Vol. 04.08). West Conshohocken, PA: ASTM International.

American Society for Testing and Materials. (2023). *Annual Book of ASTM Standards: Standard Test Methods for Compressive Strength and Elastic Moduli of Intact Rock Core Specimens under Varying States of Stress and Temperatures* (Vol. 04.09). West Conshohocken, PA: ASTM International.

American Society for Testing and Materials. (2023). *Annual Book of ASTM Standards: Standard Test Method for Bulk Density ("Unit Weight") and Voids in Aggregate* (Vol. 04.02). West Conshohocken, PA: ASTM International.

American Society for Testing and Materials. (2023). *Annual Book of ASTM Standards: Standard Test Method for Compressive Strength of Cylindrical Concrete Specimens* (Vol. 04.02). West Conshohocken, PA: ASTM International.

American Society for Testing and Materials. (2023). *Annual Book of ASTM Standards: Standard Practice for Making and Curing Concrete Test Specimens in the Laboratory* (Vol. 04.02). West Conshohocken, PA: ASTM International.

Bagherzadeh-Khalkhali, A., & Mirghasemi, A. A. (2009). Numerical and experimental direct shear tests for coarse-grained soils. *Particuology.*, *7*(1), 83-91.

Bilal, M., & Ahmad, N. (2020). Effectiveness of stone dust as an expansive soil stabilizer. *Proceedings of Conference on Sustainability in Civil Engineering (CSCE)*, (pp. 1-8). Pakistan.

Borgesson, L., Johannesson, L. E., & Gunnarsson, D. (2003). Influence of soil structure heterogeneities on the behavior of backfill materials based on mixtures of bentonite and crushed rock. *Applied Clay Science, 23*, 1-4.

Brown, G. F., Buravas, S., Charaljavanaphet, J., Jalichandra, N., Johnston, W. D., Sresthaputra, V., & Taylor, G. C. (1951). Geologic reconnaissance of the mineral deposits of Thailand. *Bulletin,* 183.

Bunopas, S (1981). *Paleogeographic history of Western Thailand and adjacent parts of Southeast Asia-A plate tectonics interpretation (Master dissertation),* University of Wellington, New Zealand.

Butcher, B. M. (1993). *The advantages of a salt/bentonite backfill for waste isolation pilot plant disposal rooms. Sandia National Laboratories,* Albuquerque, New Mexico.

Cai, Z., Zhang, D., Shi, L., Chen, Z., Chen, B., & Sun, S. (2020). Compaction and breakage characteristics of crushed stone used as the backfill material of urban pavement subsidence. *Advances in Civil Engineering, 2020,* 1-8.

Cedergren, H.R. (1989). *Seepage, drainage, and flownets.* 3rd ed, Wiley, New York, 26.

Chalermyanont, T., & Arrykul, S. (2005). Compacted sand-bentonite mixtures for hydraulic containment liners. *Songklanakarin Journal of Science and Technology, 27*(2), 313-323.

Dhir, R. K., Limbachiya, M. C., McCarthy, M. J., & Chaipanich, A. (2007). Evaluation of Portland limestone cements for use in concrete construction. *Materials and Structures, 40*(5), 459-473.

Dinku, A. (2005). The need for standardization of aggregates for concrete production in ethiopian construction industry. *Proceedings of the International Conference on African Development, Ethiopia*, 1-15.

Ghafoori, N., Spitek, R., & Najimi, M. (2016). Influence of limestone size and content on transport properties of self-consolidating concrete. *Construction and Building Materials*, *127,* 588-595.

Habib, A., Begum, M. R., & Salam, M. A. (2013). Effect of stone dust on the mechanical properties of adobe brick. *Innovative Science, Engineering & Technology, 2*(9), 631-637.

Haleerattanawattana, P. (2004). Development of cement-based ultra-high strength concrete. *Chulalongkorn University*.

Hazen, A. (1892). Filtration of water. *American Journal of Public Health*, *22*(8), 399-403.

Holtz, R. D., Kovacs, W. D., & Sheahan, T. C. (1981). Some observations regarding the strength and deformability of sandstones in dry and saturated conditions. *Bulletin of Engineering Geology and the Environment, 62,* 245-249.

Horak, E., Sebaaly, H., Maina, J., & Varma, S. (2017). Relationship between bailey and dominant aggregate size range methods for optimum aggregate packing and permeability limitation. *Southern African Transport Conference*.

Jain, A. K., Jha, A. K., & Akhtar, P. M. (2022). Assessing the swelling and permeability behavior of novel marble dust–bentonite with sand–bentonite mixes for use as a landfill liner material. *Indian Geotechnical Journal, 52*(3), 675-690.

Javanaphet, J. C. (1969). Geological map of Thailand, scale 1:1,000,000. *Department of Mineral Resources,* Bangkok, Thailand.

Johannesson, L. E., & Nilsson, U. (2006). *Geotechnical Properties of Candidate Backfill Material for Deep Repository*, *AB*, Svensk Kärnbränslehantering.

Kandolkar, S. S., & Mandal, J. N. (2016). Behavior of reinforced-stone dust walls with backfill at varying relative densities. *Hazardous, Toxic, and Radioactive Waste, 20*(1)*,* 04015010.

Kaya, A., & Durukan, S. (2004). Utilization of bentonite-embedded zeolite as clay liner. *Applied Clay Science*, *25*(1-2), 83-91.

Khamput, P. (2005). Properties of quarry dust for use as fine aggregate. *Research and Development, 16*(2)*,* 34-37.

Kim, D., & Ha, S. (2014). Effects of particle size on the shear behavior of coarse grained soils reinforced with geogrid. *Materials*, *7*(2), 963-979.

Lee, J. W., & Baek, C. (2023). Microstructure analysis and mechanical properties of backfill material using stone sludge. *Materials, 16*(4)*,* 1511.

Li, L. G., & Kwan, A. K. H. (2015). Adding limestone fines as cementitious paste replacement to improve tensile strength, stiffness and durability of concrete. *Cement and Concrete Composites*, *60*, 17-24.

Mahzuz, H. M. A., Ahmed, A. A. M., & Yusuf, M. A. (2011). Use of stone powder in concrete and mortar as an alternative of sand. *Environmental Science and Technology, 5*(5)*,* 381-388.

Mishra, A. K., Ohtsubo, M., Li, L. Y., & Higashi, T. (2010). Influence of the bentonite on the consolidation behaviour of soil–bentonite mixtures. *Carbonates and Evaporites, 25,* 43-49.

Neville, A. M. (1995). Properties of concrete. *Longman, London,* 846.

Ogila, W. A. M. (2016). The impact of natural ornamental limestone dust on swelling characteristics of high expansive soils. *Environmental earth sciences*, *75*(24), 1493.

Pastor, J. L., Tomás, R., Cano, M., Riquelme, A., & Gutiérrez, E. (2019). Evaluation of the improvement effect of limestone powder waste in the stabilization of swelling clayey soil. *Sustainability, 1,* 1-14.

Power, M. C. (1982). *Comparison Charts for Estimating Roughness and Sphericity*: AGI Data Sheets*.* Alexandria, *American Geological Institute.*

Pradeep, N., Satyanarayana, P.V.V., & Raghu P. (2013). Performance of Crusher Dust in High Plastic Gravel Soils As Road Construction Material. *Mechanical and Civil Engineering, 10*(3)*,* 1-5.

Prakash, K. S., & Rao, C. H. (2016). Study on compressive strength of quarry dust as fine aggregate in concrete. *Advance in Civil Engineering, 2016,* 1-5.

Priyanka, A. J., & Dilip, K. K. (2013). Effect of replacement of natural sand by manufactured sand on the properties of cement mortar. *Civil and Structural Engineering*, *3*(3)*,* 621-628.

Proia, R., Croce, P., & Modoni, G. (2016). Experimental investigation of compacted sand-bentonite mixtures. *Procedia Engineering.*, *158,* 51-56.

Prokopski, G., Marchuk, V., & Huts, A. (2020). Influence of limestone size and content on transport properties of self-consolidating concrete. *Construction and Building Materials, 127,* 23-49.

Pusch, R. (1998). Backfilling with mixtures of bentonite/ballast materials or natural smectitic clay.

Rajput, S. P. S., & Chauhan, M. S. (2014). Suitability of crushed stone dust as fine aggregate in mortars. *Emerging Technology and Advanced Engineering, 4*(3), 87-89.

Rajput, S. P. S. (2018). An Experimental study on crushed stone dust as fine aggregate in cement concrete. *Proceedings of Materials Today, 5*(9), 17540-17547.

Sabat, A. K., & Muni, P. K. (2015). Effects of limestone dust on geotechnical properties of an expansive soil. *Int. J. Appl. Eng. Res*, *10*(1), 377724-37730.

Sabat, A. K., & Nanda, R. P. (2011). Effect of marble dust onstrength and durability of Rice husk ash stabilised expansive soil. *Civil & Structural Engineering*, *1*(4), 939-948.

Satyanarayana, P. V. V., Varma, N. S. C., Chaitanya, D. K., & Raj, P. G. (2016). A study on performance of crusher dust in place of sand as a sub-grade and fill material in geo-technical applications. *Advance Civil Engineering Research, 1*(1), 1-11.

Satyanarayana, P.V.V., Prem Teja, R., Harshanandan, T., & Lewis Chandra, K. (2013). A study on the use of crushed stone aggregate and crusher dust mixes in flexible pavements. *Scientific & Engineering Research, 4*(11), 1126.

Saygili, A. (2015). Use of Waste Marble Dust for Stabilization of Clayey Soil. *Materials Science, 21,* 601-606.

Singh, A. K., Srivastava, V., & Agarwal, V. C. (2015). Stone dust in concrete: effect on compressive strength. *Engineering and Technical Research, 3*(8), 115-118.

Sobti, J., & Singh, S. K. (2017). Hydraulic conductivity and compressibility characteristics of bentonite enriched soils as a barrier material for landfills. *Innovative Infrastructure Solutions, 2*, 1-3.

Soltani-Jigheh, H. & Jafari, K. (2012). Volume change and shear behavior of compacted clay-sand/gravel mixtures. *Engineering and Applied Sciences, 4*, 52-66.

Sperry, M. S., & Peirce, J. J. (1995). A model for estimating the hydraulic conductivity of granular material based on grain shape, grain size and porosity. *Ground Water, 33*(6), 892-898.

Sridharan, A., Soosan, T. G., & Babu, T.J. (2005). Utilization of quarry dust to improve the geotechnical properties of soils in highway construction. *Canadian Geotechnical Journal, 28,* 391-400.

Sridharan, A., Soosan, T. G., Babu, T.J., & Abraham B. M. (2006). Shear strength studies on soil-quarry dust mixtures. *Geotechnical Engineering*, *24*, 1163-1179.

Srikanth, V., & Mishra, A. K. (2016). A laboratory study on the geotechnical characteristics of sand–bentonite mixtures and the role of particle size of sand. *Geosynthetics and Ground Engineering*, *2*(3), 1-10.

Suman, B. K. (2018). Suitability of Stone Dust in Concrete. *Engineering Development and Research, 6*(2)*,* 629-633.

Suman, B. K., Singh, A. K., & Srivastava, V. (2015). Stone dust as fine aggregate replacement in concrete: effect on compressive strength. *Advances in Engineering and Emerging Technology, 7*(4), 220-224.

Suwansukrot, N. (2007). Compressive strength of concrete using different sizes of stone. *Khon Kaen University*.

Thanh Duong, N., & Van Hao, D. (2020). Consolidation characteristics of artificially structured kaolin-bentonite mixtures with different pore fluids. *Advances in Civil Engineering, 2020,* 1-9.

Thongsanitgarn, P., Wongkeo, W., Sinthupinyo, S., & Chaipanich, A. (2011). Effect of limestone powders on compressive strength and setting time of Portland-Limestone Cement Pastes. *Proceedings of TIChE International Conference*, 1-4.

Tonnayopas, D., Kaewsomboon, W., & Jantaramanee, S. (2009). Characterization of ceramic tile fabricated from basalt quarry dust incorporated with oil palm fiber ash. *Proceedings of Thaksin University annual conference, 12,* (pp. 149-159). Thailand.

Van Lopik, J. H., Zazai, L., Hartog, N., & Schotting, R. J. (2020). Nonlinear flow behavior in packed beds of natural and variably graded granular materials. *Transport in Porous Media, 131,* 957-983.

Vangla, P., & Latha, G.M. (2015). Influence of particle size on the friction and interfacial shear strength of sands of similar morphology. *Geotechnical Engineering, 733*, Englewood Cliffs, NJ: Prentice-Hall.

Wakchaure, M. R., Shaikh, A. P., & Gite, B. E. (2012). Effect of Types of Fine Aggregate on Mechanical Properties of Cement Concrete. *Modern Engineering Research*, *2*(5), 3723-3726.

Yalley, P. P., & Sam, A. (2018). Effect of sand fines and water / cement ratio on concrete properties. *Civil Engineering Research*, *4*(3), 1-7.

Yanrong, L. (2013). Effects of particle shape and size distribution on the shear strength behavior of composite soils. *Bulletin of Engineering Geology and the Environment*, *72*(3-4), 371-381.
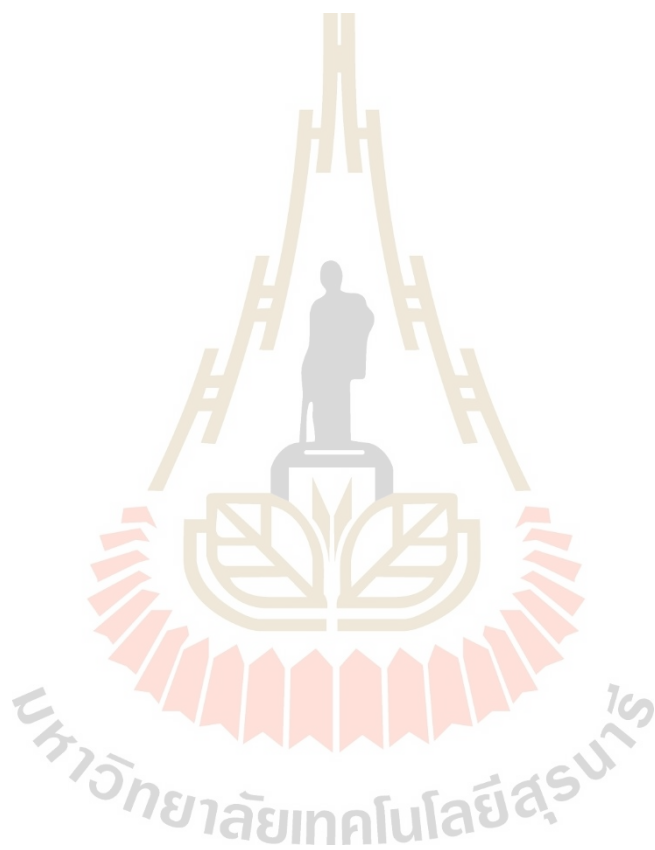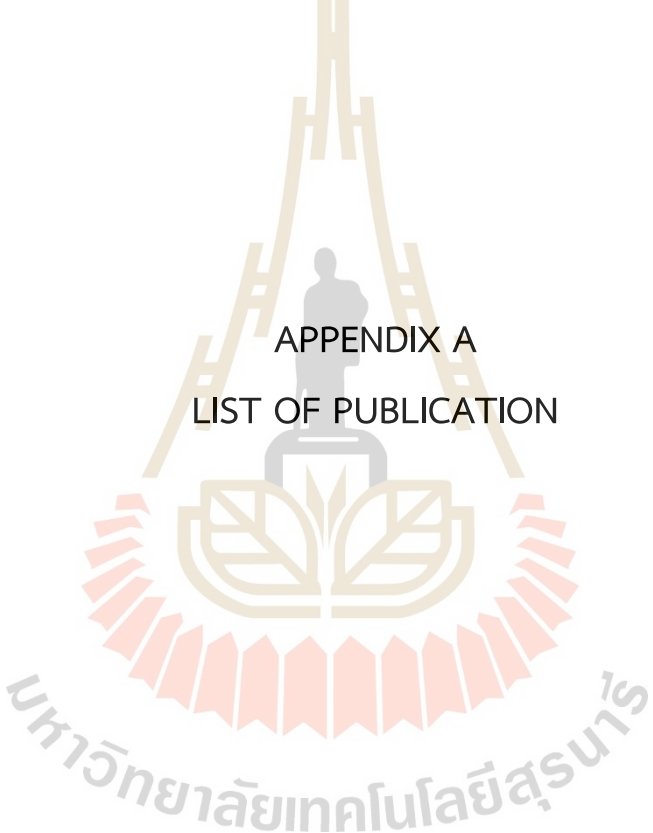
APPENDIX A

LIST OF PUBLICATION

Application of stone dust for cement and bentonite mixtures

Jadsadakorn Sripiyaphan[1*], Kittitep Fuenkajorn[1]

[1]Geomechanics Research Unit, Suranaree University of Technology, Nakhon Ratchasima 30000, Thailand

*Jadsadakorn.sri@gmail.com

Abstract — **The objective of this study is to determine the potential applications of stone dust for cement and bentonite mixtures. Results indicate that stone dust with particle size ranges of 0.25 mm and larger is suitable for cement mixtures as they show compressive strength and elastic modulus values comparable to the cement- fine sand mixtures. The particle size ranges of 0.25 mm and finer are suitable for hydraulic containment applications. The weight ratio of stone dust to bentonite of 40% is recommended as its mixtures show the highest dry density, and frictional resistance with lowest optimum water content. Results from swelling test also support that at 40% stone dust content the swelling capacity of its mixtures is about 50% of that of pure bentonite. The separator between coarse and fine grained stone dust at 0.25 mm allows the applications stone dust to construction industry and hydraulic containment work.**

Keywords — **compressive strength, compaction, swelling, direct shear.**

I. INTRODUCTION

Stone dust is a waste product produced by limestone crushing plants during the process of producing coarse aggregates of various sizes. The workability, compressive strength, and optimum moisture content of stone dust with coarse particles is not significantly different from clean sand [1]. It is a good substitute material to reduce reserves and reduce the shortage of natural materials [2]. Utilization of the stone dust for other purposes is being considered in order to reduce the volume of the stone dust. These solutions include mixing stone dust with cement for use in the foundation, fill material [3], backfill material [4], flexible pavement [5], reinforced-stone dust walls [6], construction materials such as brick block [7] and ceramic tile fabricated [8]. To reduce permeability in the fractured rock mass, a common solution used internationally in the construction industry is to use bentonite mixed with cement as a grouting material. The use of stone dust to minimize groundwater flow in rock fractures is another solution to the problem. Depending upon different regions in Thailand, stone dust is not truly acceptable in the locations where clean sand is vastly available (e.g., west and southeast of the country). Nevertheless, in the northeast of Thailand stone dust is well acceptable as a substitute of clean sand because the sand is not widely available. Care should, however, be taken to ensure that the particle size ranges, chemical compositions, particle shapes are suitable for substitution of the commonly used materials.

The objectives of this study are to assess the mechanical properties of stone dust mixed with Portland cement and hydraulic containments of stone dust mixed with bentonite for industrial use. The main tasks include particle size analysis, X-ray diffraction analysis, uniaxial compression test, compaction test, direct shear test, consolidation test, and swelling test.

II. CHARACTERIZATION OF STONE DUST

The stone dust used in this study is prepared from Khumngern Khum-tong Co., Ltd., stone crushing plant in Nakhon Ratchasima province. It has a bulk density of 1.62 g/cc, which is determined by the ratio of dry mass and volume, following the ASTM C29/C29M-17 standard [9]. Mineral compositions of the stone dust specimens are analyzed by X-ray diffraction (XRD). The XRD specimen is prepared by crushing the stone dust to obtain rock powder with particle sizes less than 0.25 mm (mesh #60). Using X-ray diffraction (Bruker, D2 Phaser), following the ASTM E1426-14e1 standard practice [10]. The results are given in Table 1, showing the stone dust composes mainly of calcite (67%), dolomite (26%) and minor amounts of trace minerals.

Grain size analysis is performed to determine the percentage of particle sizes obtained by sieve analysis. The stone dust particle sizes are classified using sieve nos. 4, 10, 20, 40, 60, 100 and 200. Cumulative curves are constructed based on weight percent, as shown in Fig.1 The test method and calculation follow the ASTM C136–06 standard [11].

The sphericity and roughness are determined from individual particles which are divided into 7 particle size ranges, including 4.75, 2.0, 0.85, 0.425, 0.25, 0.15 and 0.075 mm. Ten particles are examined for each size range, using an optical microscope. Based on the widely used classification systems given by Powers [12], the averages of the roughness and sphericity for each material are shown in Table 2.

Table 1 Mineral compositions of stone dust from XRD analysis.

Mineral Compositions	Weight (%)
Calcite	66.92
Dolomite	25.97
Ankerite	3.51
Huntite	1.61
Cooperite	0.18
Cuspidine	1.12
Natron (Soda)	0.69

Table 2 Particle shape classification for stone dust particles based on Powers [12].

Particle size (mm)	Roundness	Sphericity	Classification	
4.75	0.37	0.48	Subrounded	Low sphericity
2.0	0.46	0.77	Subrounded	
0.85	0.51	0.57	Rounded	
0.425	0.43	0.80	Subrounded	
0.25	0.49	0.91	Subrounded	
0.15	0.41	0.77	Subrounded	
0.075	0.74	1.00	Well rounded	

The entire particle size range is separated into 2 parts. This is primarily to be more practical and economic for industry, where only one separator is required at the end of the conveyer belt that carries the stone dust from the rock crusher to the stockpile. In the study, two sets of size separations are used as shown in Fig.1. For the first separator, particles within ranges of 4.75-0.25 mm are considered coarse particles, while those within the ranges of 0.25-0.075 mm are categorized as fine particles. For the second separator, particles ranging from 4.75-0.150 mm are coarse, and those within the range of 0.150-0.075 mm are fine.

The coarse particles are applied for cement mixture, and the fine ones are for bentonite mixture. The mixture strength will be used as an indicator of which size separators would be more appropriate between strength application and hydraulic containment application.
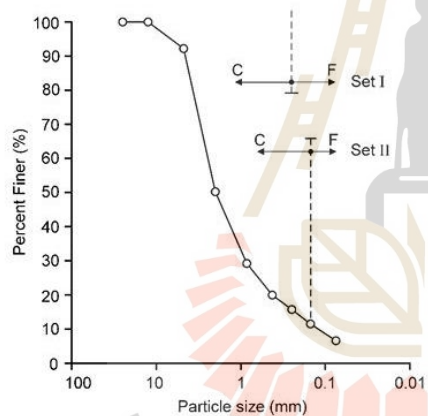
Fig. 1 Particle size ranges separated for cement mixtures and bentonite mixtures. C is coarse particles and F is fine particles.

III. CEMENT-STONE DUST MIXTURES

To determine the mechanical properties of cement-stone dust mixtures, the cement Portland cement type I, is used with ratio of the stone dust to cement (SD:C) set as 2:1 and water-cement (W:C) ratio of 1:0.5 by weight, following the ASTM C39 standard [13]. A cement mixer is used to prepare the specimen to obtain a consistent slurry. The slurry of all mixtures is poured into cement cast with diameter and length of 15 and 30 cm. The curing time is 7 days. The mixing and pouring into cement cast is performed in accordance with ASTM C192 standard [14].

Compression Test

The mechanical properties of the specimens are determined after 7 days of curing. The specimen compressive strengths are determined by axially loading under constant rate of 0.1 MPa/second until failure. The axial and lateral displacements are monitored. The compressive strength, elastic modulus and Poisson's ratio are determined in accordance with the ASTM D7012-14e1 standard practice [15]. The post-failure characteristics are observed and recorded.

The test results show that the compressive strengths and elastic moduli are highest for particle sizes of 4.75-0.25 mm (set I). The strengths and elastic moduli are higher than those mixed with clean sand (Fig. 2). The Poisson's ratio tends to be similar for all specimens, suggesting that the particle size ranges do not affect the specimen dilation.

A comparison of the coarse particles between set I and set II reveals that the particles in set I (4.75-0.25 mm) are suitable as cement mixture materials and substitute for clean sand in the cement mix.

IV. BENTONITE-STONE DUST MIXTURES

The particle sizes of less than 0.25 mm (set I) are used here to mix with bentonite for hydraulic containment application. They are subjected to basic tests described are follows.

Compaction Test

The fine-grained stone dust is mixed with bentonite using percentages of bentonite of 100, 80, 60, and 40% by weight. The mixtures are prepared in stainless steel tray using 2.7 kilograms of the mixture. Water is added on the mixture until the desired water content is reached. They are mixed thoroughly using a spatula. The samples compacted with a release of weight steel hammer 10 pounds in mold of 25 times per layer for five layers in the mold, following ASTM D698 standard method [16].

The results show the maximum dry unit weight as a function of water weight ratios in Fig. 3. The increase of the maximum dry unit weight with increasing stone dust weight ratios, where the mixtures after compaction have higher unit weight than those before compaction. The optimum water contents decrease with the bentonite weight ratio.
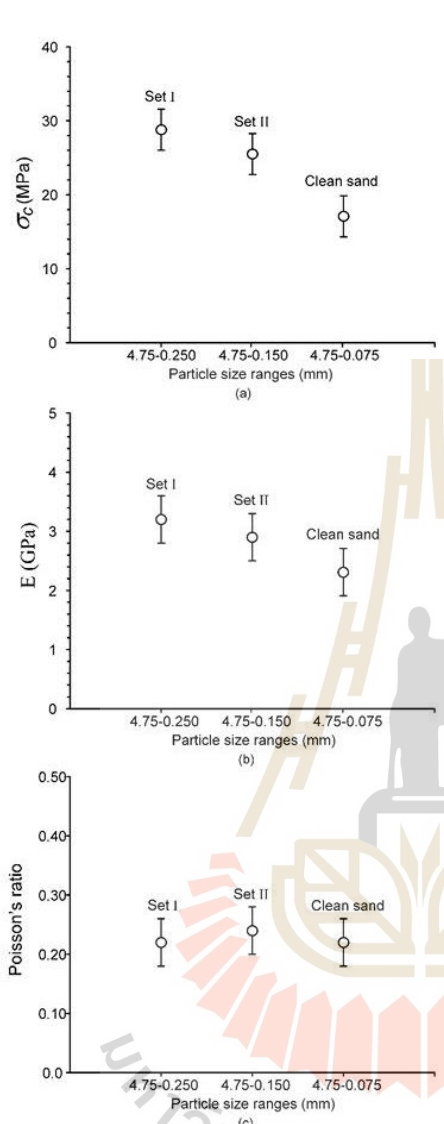
Fig. 2 Compressive strengths (a), elastic modulus (b) and poisson's ratio (c) of cement-stone dust mixtures with 7 days curing.
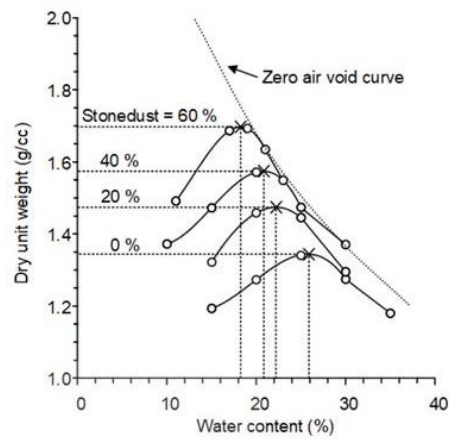
Fig. 3 Maximum dry density as a function of water content for various stone dust-bentonite mixing rations for the first separator (set I).

Direct shear Test

The direct shear test is performed to investigate maximum shear strengths of bentonite-stone dust mixture with the optimum water content. After compaction process, specimens are trimmed by Soil Trimmer, then put into a stainless shear box. A hydraulic load cell is used for applying shear force. The used normal stresses constants are 25, 50, 75 and 100 psi by dead load. The shear stress is applied. The shear displacement and dilation are read for every 0.01 mm.

Fig. 4 shows the results shear stresses increase with shearing displacement, particularly when are high normal stresses. The amount of dilatation increases significantly as aggregate particle size increases. The shear strength and normal stress curves are shown in Fig. 4. Shear strength increases linearly with normal stress in all mixtures.

The mixtures with lower percentages of bentonite show greater shear strengths than those with higher percentages of bentonite. The cohesions and friction angles of specimens mixtures are plotted in Fig. 5. It's clear that increasing the fine-grained stone dust decreases the cohesions. While percentage of bentonite decreasing, the friction angles increase. This may be due to the greater frictional resistance between the grain surfaces of the stone dust mixture.

Consolidation Test

Consolidation tests are performed on the mixtures under previously obtained optimum water content. The applied of constant axial stresses using hydraulic load cell range from 10, 20, 40, 80, 160, 320, 640, to 1280 kPa for 10 days. The axial displacements are recorded with high precision gages.
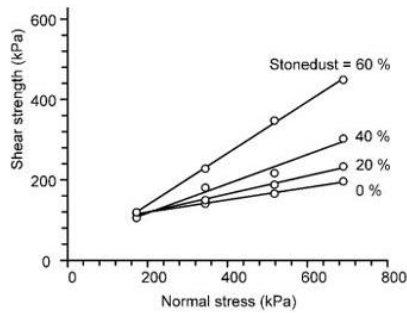
Fig. 4 Shear strengths as a function normal stress for the first separator (set I).
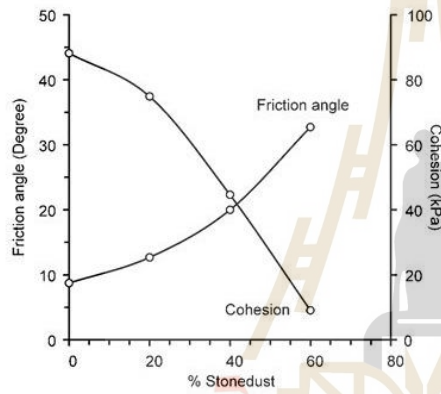
Fig. 5 The cohesions and friction angles of specimens mixtures for the first separator (set I).

The cumulative pore volume decreases with increasing fine grained stone dust percentage, as a shown in Fig. 6. The settlement of fine-grained stone dust-bentonite mixtures decreases when percentage of fine-grained stone dust increases. This is because of the pore filling phenomena, which occurs with addition of bentonite particles to fine grained stone dust. The bentonite particles can penetrate inside the void spaces created by the fine-grained stone dust, and hence stiffening the specimens matrix.

Swelling Test

The weight ratios of fine-grained stone dust-bentonite from 0:100, 20:80, 40:60 and 60:40 are studied. After compaction at optimum water content, the top surface is trimmed to obtain smooth surface. The brass (porous stone) is placed on the top of the sample. The sample is submerged under water. The readings are made every minute for the first haft hour. After that the reading intervals gradually increase to every hour. Swelling test method follows ASTM D4546-08 standard [17].

Swelling ratio by various bentonite weight ratios are shown in Fig. 7. The results indicated that the maximum swelling ratio increased with increasing the bentonite weight ratio. This is because bentonite characteristically swells into water many times its dry volume. The swelling increases rapidly within the 6 days, except for the samples with of 0:100 and 20:80. They fluctuate until 10 days and tend to remain constant for all weight ratio after 30 days.
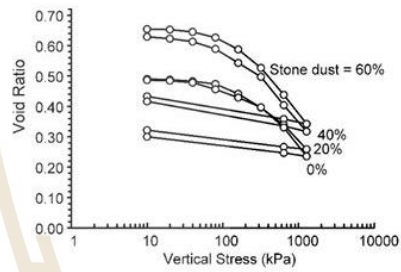
Fig. 6 Void ratio versus effective stress of fine-grained stone dust-bentonite mixtures for the first separator (set I).
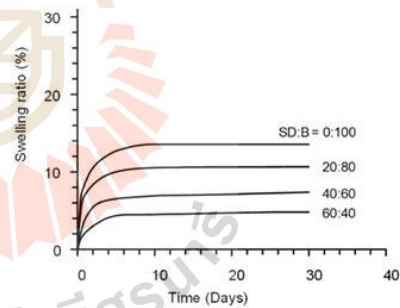
Fig. 7 Swelling ratio as a function of time for the first separator (set I).

V. DISCUSSIONS AND CONCLUSIONS

This study determines the potential application of stone dust used for cement and bentonite mixtures. The stone dust is separated into coarse and fine particles, where only one separator can be installed between the rock crusher and the stockpile. Two sets of size separations are selected. Set I, particles within the ranges of 4.75-0.25 mm are considered coarse, while those within the range of 0.25-0.075 mm are classified as fine. Set II, particles sized 4.75-0.15 mm are considered coarse, and those within the range of 0.150-0.075 mm are classified as fine. The coarse particles are used for cement mixture, while the fine particles are used for the bentonite mixture.

The compressive strengths and elastic modulus results for cement mixture show that the coarse particles from set I (4.75-0.25 mm) have greater strength as compared to those from set II (4.75-0.150). This trends again supported the investigations obtained elsewhere [18]. This is because concrete with higher fines content absorbs more water during the hydration leading to the decrease of strength. This can be fulfilled by optimizing the volume percentage of different grain sizes within the stone dust. As a result, the separation in set I is suitable for substituting clean sand. Only the fine particles from set I (0.25-0.075 mm) are therefore considered for the bentonite mixture.

The small particles can fill the pore spaces between cement particles in the paste better than the larger ones which is known as filling effect. The fineness of stone dust has influence on the observed compressive strength values [19]. Porosity is a very important factor that affects the behavior of specimens, lower porosity leading to greater uniaxial compressive strength and Young's modulus [20], [21]. A smaller grain size might affect however the strength of sample. This can be done by optimizing the mixed grain size of stone dust volume percentage. [22].

Compaction, direct shear, consolidation, and swelling tests are conducted on mixtures of bentonite and fined stone dust to obtain the optimal ratio. The test results show that the increase of the stone dust weight ratio increases the dry unit weight and decreases the optimum water content. This agrees reasonably well with the test results obtained by [23]-[26]. The mixtures containing 60% stone dust exhibit the highest shear strength and friction angle, while displaying the lowest cohesion, settlement, and swelling behavior. This is attributed to the effective filling of small void spaces by the fine particles, resulting in an increase of shear strength. Lower bentonite contents contribute to reduction of swell capacity. A mixture of 40% bentonite and 60% stone dust may be suitable because it shows the highest maximum dry unit weight, shear strengths, and can decrease the cost of the bentonite materials. As suggested by [27]-[29], that for effective compaction the bentonite weight ratio for the mixtures should not be less than 30%. This is primarily to prevent bridging and voids occurring between aggregates particles.

REFERENCES

[1] P. Khamput, "Properties of quarry dust for use as fine aggregate," *Research and development*. Vol.16, no.5, pp.34-37, 2005.

[2] K. S. Prakash, and C. H. Rao, "Study on compressive strength of quarry dust as fine aggregate in concrete," *Advances in Civil Engineering*. Vol.2016, pp.1-5, 2016.

[3] P. V. V. Satyanarayana, N. S. C. Varma, D. K. Chaitanya, and P. G. Raj, "A Study on performance of crusher dust in place of sand as a sub-grade and fill material in geo-technical applications," *Advanced Civil Engineering Research*. Vol.1, no.1, pp.1-11, 2016.

[4] Z. Cai, D. Zhang, L. Shi, Z. Chen, B. Chen, and S. Sun, "Compaction and breakage characteristics of crushed stone used as the backfill material of urban pavement subsidence," *Advances in Civil Engineering*. pp.1-8, 2020.

[5] P. V. V. Satyanarayana, R. Prem Teja, T. Harshanandan, and K. Lewis Chandra, "A study on the use of crushed stone aggregate and crusher dust mixes in flexible pavements," *Scientific & Engineering Research*. Vol.4, no.11, pp.1126, 2013.

[6] S. S. Kandolkar, and J. N. Mandal, "Behavior of reinforced-stone dust walls with backfill at varying relative densities," *Hazardous, Toxic, and Radioactive Waste*. Vol.20, no.1, pp.04015010,2016.

[7] A. Habib, M. R. Begum, and M. A. Salam, "Effect of stone dust on the mechanical properties of adobe brick," *IJISET—Int J Innov Sci Eng Tech 2*. Vol.2, no.9, pp.631-637,2013.

[8] D. Tonnayopas, W. Kaewsomboon, and S. Jantaramanee, "Characterization of ceramic tile fabricated from basalt quarry dust incorporated with oil palm fiber ash," *in Proc. Thaksin University annual conference*, 2009, paper 12, p. 149-159.

[9] ASTM C29/C29M-97, *Standard Test Method for Bulk Density ("Unit Weight") and Voids in Aggregate*, In Annual Book of ASTM Standards, West Conshohocken, PA,1997.

[10] ASTM E1426-14, *Standard Test Method for Determining the X-Ray Elastic Constants for Use in the Measurement of Residual Stress Using X-Ray Diffraction Techniques*, In Annual Book of ASTM Standards, West Conshohocken, PA,2019.

[11] ASTM C136-06, *Standard Test Method for Sieve Analysis of fine and Coarse Aggregate*, In Annual Book of ASTM Standards, West Conshohocken, PA,2006.

[12] M. C. Power, *Comparison Charts for Estimating Roughness and Sphericity*, AGI Data Sheets, American Geological Institute, Alexandria, 1982

[13] ASTM C39/C39M-14, *Standard Test Method for Compressive Strength of Cylindrical Concrete Specimens*, In Annual Book of ASTM Standards, West Conshohocken, PA,2014.

[14] ASTM C192/C192M-00, *Standard Practice for Making and Curing Concrete Test Specimens in the Laboratory*, In Annual Book of ASTM Standards, West Conshohocken, PA,2000.

[15] ASTM D7012-14, *Standard Test Methods for Compressive Strength and Elastic Moduli of Intact Rock Core Specimens under Varying States of Stress and Temperatures*, In Annual Book of ASTM Standards, West Conshohocken, PA,2014.

[16] ASTM D698-07, *Standard Test Methods for Laboratory Compaction Characteristics of Soil Using Standard Effort*, In Annual Book of ASTM Standards, West Conshohocken, PA,2007.

[17] ASTM D4546-08, *Standard Test Methods for One-Dimensional Swell or Collapse of Cohesive Soils*, In Annual Book of ASTM Standards, West Conshohocken, PA,2008.

[18] P. P. Yalley, and A. Sam, "Effect of sand fines and water / cement ratio on concrete properties," *Civil Engineering Research.*, Vol. 4, no.3, pp. 1-7,2018.

[19] P. Thongsanitgarn, W. Wongkeo1, S. Sinthupinyo, and A. Chaipanich, "Effect of limestone powders on compressive strength and setting time of Portland-Limestone Cement Pastes," in Proc. *TIChE International Conference*, 2011, p.1-4.

[20]   V. Srikanth, and A. K. Mishra, "A laboratory study on the geotechnical characteristics of sand-bentonite mixtures and the role of particle size of sand," *Geosynth. and Ground Eng.*, Vol. 2, pp. 1-10, 2016.

[21]   N. Ghafoori, R. Spitek, and M. Najimi, "Influence of limestone size and content on transport properties of self-consolidating concrete," *Construction and Building Materials.*, Vol. 127, pp.588-595, 2016.

[22]   G. Prokopski, V. Marchuk, and A. Huts, "The effect of using granite dust as a component of concrete mixture," *Case Studies in Construction Materials.*, Vol. 13, pp. 1-7, 2020.

[23]   M. Bilal, and N. Ahmad, "Effectiveness of stone dust as an expansive soil stabilizer," in Proc. *Conference on Sustainability in Civil Engineering (CSCE)*, 2020, p. 1-8.

[24]   J. L. Pastor, R. Tomás, M. Cano, A. Riquelme, and E. Gutiérrez, "Evaluation of the improvement effect of limestone powder waste in the stabilization of swelling clayey soil," *Sustainability.*, Vol. 11, pp. 1-14,2019.

[25]   N. Ural, and B. Görgün, "Effect of different sands on one-dimensional and hydraulic consolidation (radial) tests of clay," *Iran J Sci Technol Trans Civ Eng.*, Vol. 43, pp. 331-341,2019.

[26]   N. T. Duong, and D. V. Hao, "Consolidation characteristics of artificially structured kaolin-bentonite mixtures with different pore fluids," *Advances in Civil Engineering.*, Vol. 2020, pp. 1-9,2020.

[27]   B. M. Butcher., The Advantages of A Salt/Bentonite Backfill for Waste Isolation Pilot Plant Disposal Rooms," Sandia National Laboratories, Albuquerque, New Mexico, 1993.

[28]   L. Borgesson, L. E. Johannesson, and D. Gunnarsson, "Influence of soil structure heterogeneities on the behavior of backfill materials based on mixtures of bentonite and crushed rock," *Applied Clay Science.* Vol. 23(1-4), pp. 121-131.2003.

[29]   L. E. Johannesson, and U. Nilsson, "Geotechnical Properties of Candidate Backfill Material for Deep Repository," AB, Svensk Kärnbränslehantering,2006.

BIOGRAPHY

Ms. Jadsadakorn Sripiyaphan born on July 3, 1997 in Nakhon Ratchasima, Thailand. He received his Bachelor's Degree in Engineering (Geological Engineering) from Suranaree University of Technology in 2020. For her post-graduate, he continued to study with a Master's degree in the Geological Engineering Program, Institute of Engineering, Suranaree university of Technology. During graduation, 2020-2023, He was a part time worker in position of research associate at the Geomechanics Research Unit, Institute of Engineering, Suranaree University of Technology.